

|  |   |   |         |
|--|---|---|---------|
| <i>MANUSCRIT ACCEPTAT</i>  |   |  |         |
| <b>Establishing a new reference group of Keay 25.2 amphorae from Sidi Zahrani (Nabeul, Tunisia)</b>  |   |   |         |
| S. Baklouti ; L. Maritan ; Ll. Casas ; N. Laridhi Ouazaa ; R. Jàrrega ; M. Prevosti ; C. Mazzoli ; B. Fouzaï ; S. Larabi Kassaa ; M. Fantar  |   |   |         |
| <b>Revista</b>   | <a href="#">Applied Clay Science. Volume 132-133</a> , November 2016, Pages 140-154                 |   |         |
| <b>DOI</b>   | <a href="https://doi.org/10.1016/j.clay.2016.05.027">https://doi.org/10.1016/j.clay.2016.05.027</a> |   |         |
| <b>Disponible en línia</b>   | 6/6/2016  | <b>Data de publicació</b>   | 11/2016 |
| Per citar aquest document:<br><br>S. Baklouti, L. Maritan, Ll. Casas, N. Laridhi Ouazaa, R. Jàrrega, M. Prevosti, C. Mazzoli, B. Fouzaï, S. Larabi Kassaa, M. Fantar, Establishing a new reference group of Keay 25.2 amphorae from Sidi Zahrani (Nabeul, Tunisia), In Applied Clay Science, Volumes 132–133, 2016, Pages 140-154, ISSN 0169-1317, <a href="https://doi.org/10.1016/j.clay.2016.05.027">https://doi.org/10.1016/j.clay.2016.05.027</a> . |   |   |         |
| Aquest arxiu PDF conté el manuscrit acceptat per a la seva publicació.   |   |   |         |

## Abstract

This paper presents the results of the archaeometric study of African Keay 25.2 amphorae from the archaeological site of Sidi Zahruni (Beni Khair, NE Tunisia), where this pottery was massively produced. A set of 43 amphorae was analysed with a combined approach consisting of thin-section petrography, X-ray powder diffraction (XRPD) and X-ray fluorescence (XRF), to establish a homogeneous reference group for this production. Although all the amphorae are petrographically very similar, three petro-fabrics were identified in terms of grain-size distribution and abundance of inclusions. Detailed digital image analysis, carried out on SEM-BSE images of some representative samples of each petro-fabric, was used to quantify the differences among them. Cluster analysis of XRPD data patterns also revealed groups of samples for which similar raw materials/paste and firing conditions were used, contributing to better assessment of information on the production process. Statistical multivariate treatment (principal component and cluster analyses) of chemical data and comparisons with 10 samples previously attributed to the Sidi Zahruni potteries show that the potsherds analysed here are similar from the geochemical viewpoint. Similar trends in the abundance and ratio of some trace and rare earth elements (REE) also indicate that the Sidi Zahruni amphorae were produced from a local clayey material collected from nearby outcrops of Upper Miocene deposits.

## Highlights

- Archaeometric study of African Keay 25.2 amphorae from Sidi Zahruni site, north-eastern Tunisia.
- Comparisons of both bulk chemical composition and trace and rare earth element (REE) patterns of both studied amphorae and those from literature data with local clayey materials allow defining the area from which the clay was supplied at Sidi Zahruni.
- New and consistent “reference group” for Keay 25.2 amphorae is established for Sidi Zahruni.

## Keywords

Petro-groups ; Chemical data ; Reference group ; Amphorae ; Roman times ; North Africa

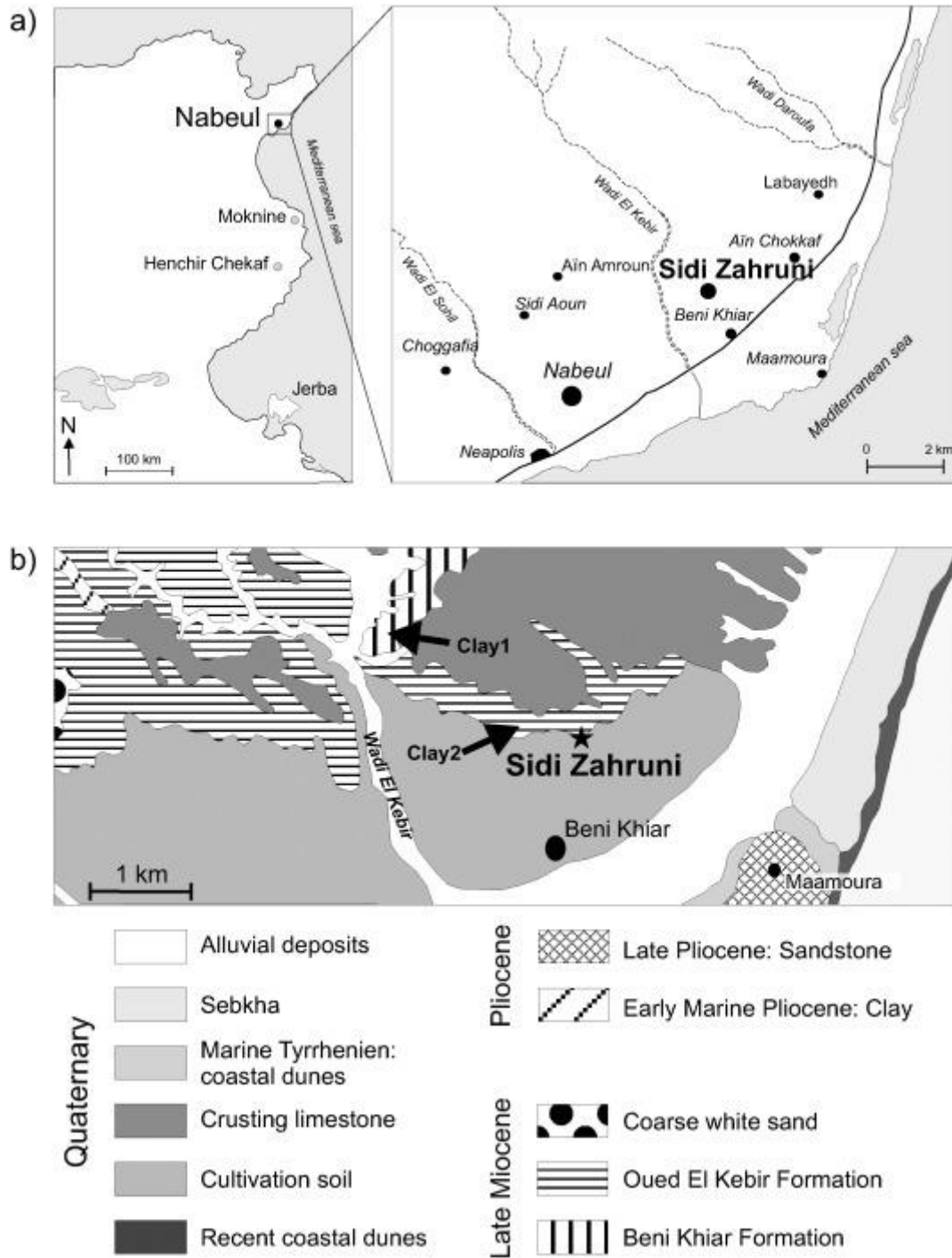
## 1. Introduction

In the last few decades, Roman amphorae have been archaeometrically investigated in several studies, and have provided valuable insights into socio-economic relations, revealing interactions between different regions (mainly trade routes) and the technological evolution of societies ([Buxeda i Garrigós et al., 2002](#); [Prudêncio et al., 2003, 2009](#); [Capelli, 2005](#); [Dias et al., 2010](#); [Fantuzzi et al., 2015a,b](#) and references therein). Problems regarding the provenance of amphorae, due to imitations, export of raw materials and potters' movements, all require the support of petrographic, chemical and mineralogical analysis in addition to classical archaeological methods based on epigraphic and typological studies. Moreover, the definition of reference groups, based on materials collected from the production site, is essential to infer the provenance of amphorae found in consumption sites.

During the Roman Empire, what is now Tunisia (once part of the Roman Province of Africa Proconsularis) was a major centre of production of African-type amphorae, which were extensively traded throughout the ancient world ([Peacock et al., 1990](#)). This type of pottery provides clear information attesting to the importance of the main economic connections among Roman regions, as trade routes were essential for transporting foodstuffs ([Bes, 2007](#)).

The paste of African amphorae is coarse enough to allow petrographic and mineralogical examination before chemical analyses. This approach has already been used on African materials from consumer sites ([Peacock, 1984, 1994](#)), on non-African materials ([Schuring, 1984](#)) and on amphorae from production sites in regions with a single source of raw materials ([Peacock and Tomber, 1991](#)). Most of the ceramics produced in North Africa, but also in Palestine, are distinguished from other Mediterranean productions by the occurrence of aeolian quartz grains in the paste. But, the lack of specific petrographic markers is a significant complication in determining the provenance of African ceramics. In some cases, the distinction among African pastes, representing specific productions, has been achieved by comparison of petrographic characteristics, typological classifications and reference groups of available workshops ([Fantuzzi et al., 2015a,b](#) and references therein). However, the widespread occurrence of similar siliciclastic lithologies in North African regions, i.e., the coarser fraction in clayey materials and sand clasts mostly composed of quartz and non-diagnostic accessory inclusions (feldspar, limestone, sandstone, clay pellets), hinder definite attribution of amphorae to specific production centres in Tunisia ([Fantuzzi et al., 2015a,b](#) and references therein). Therefore, provenance studies of amphorae from these regions also require chemical data from a significant number of samples, and statistical multivariate analysis ([Baxter, 1994](#)).

The aim of this paper is to establish a reference group, based on petrographic, mineralogical and chemical data, for a distinct class of amphora, African Keay 25.2, representing the prevalent type made at Sidi Zahrani, in the Nabeul region (NE Tunisia) ([Fig. 1a](#)). Despite the large diffusion of this amphora type in the numerous localities of the ancient Roman world, only preliminary archaeological and archaeometric studies have been carried out on these amphorae in the last decade ([Sherriff et al., 2002a,b; Fantuzzi et al., 2015a,b](#) and references therein) and they are still generally based only on the petrographic analysis of a small number of samples supplied from Sidi Zahrani and other sites of the Nabeul region. Only [Fantuzzi et al. \(2015a,b\)](#) characterised the amphorae also from a chemical viewpoint, but the amphorae they analysed were found in other Roman provinces and were attributed, on the basis of archaeological considerations, to the site of Sidi Zahrani. Proper reference groups for amphorae produced in the various localities of this region, is actually missing, and provenance attributions are at the moment based only on materials supposed to come from the production sites.



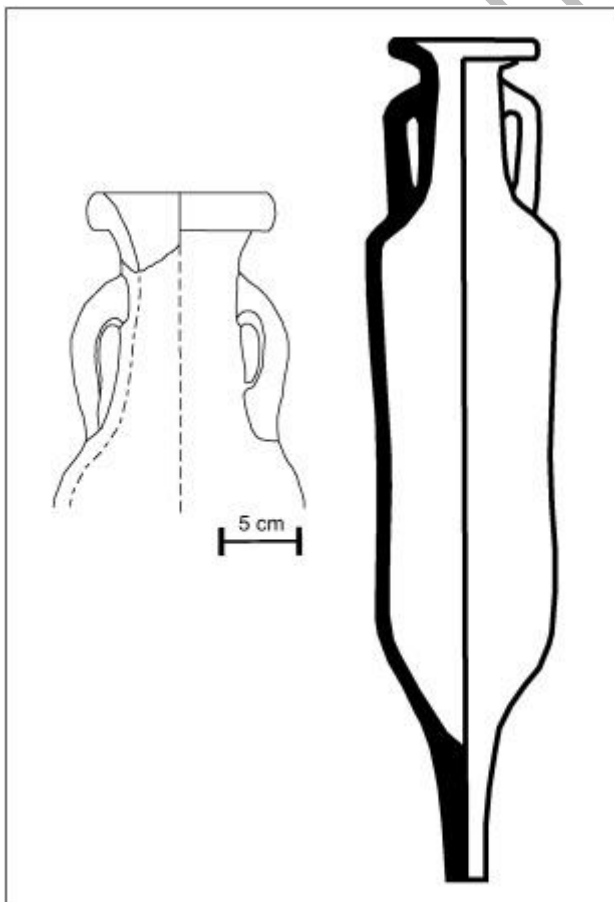
1. [Download high-res image \(797KB\)](#)
2. [Download full-size image](#)

Fig. 1. a) Location of the production centre of Sidi Zahruni in Tunisia. Other productive sites of Late Roman amphorae in north and central Tunisia are also given; b) Geological sketch of the area of Sidi Zahruni and location of clay sampling points near the site.

The archaeometric analyses here proposed will allow defining a homogeneous compositional reference group for Keay 25.2 amphorae at Sidi Zahruni. Moreover, the comparisons with clays outcropping in the area also aimed at identifying the specific source of the raw materials.

## 2. Archaeological context

One of the best-documented amphora production area in Africa Proconsularis is that of Nabeul (ancient Neapolis, NE Tunisia), where potteries have also been identified by the stamp C.I.N. [*C (olonia) I (ulia) N (eapolis)*] found on African amphorae of Africana II C (Keay, 1984). In the late 3rd/early 4th century, the classical Africana I and Africana II types were replaced by the cylindrical medium-sized Africana III (or Keay 25) type, which became the most common in the Roman world (Keay, 1984). The African Keay 25 amphora, as classified by Keay (1984) based on discoveries in Catalan sites (NE Spain), and corresponding to Africana amphorae III (Peacock et al., 1989), is a variety of the North African amphorae produced between the 4th and 7th centuries AD. This product, and particularly its most common variant Keay 25.2 (Fig. 2), corresponding to Africana III C (Fantuzzi et al., 2015a,b and references therein), has been found in many regions of Tunisia, mainly in Zeugitana (Nabeul) and Byzacena (Sullectum, Thaenae, Oued El Akarit) where many potteries have been discovered (Peacock et al., 1989). Archaeological surveys of the Nabeul region have shown the existence of many Roman potteries such as Aïn Amroun, Sidi Zahruni, Sidi Aoun, Briquéteries (Fantuzzi et al., 2015a,b and references therein), Choggafia, Aïn Chokkaf, Labayedh, and many others located near villages. The most important of these is that of Sidi Zahruni (Fig. 1a), with large-scale ceramic production dominated by amphorae, and active mainly between the 5th and 7th centuries AD. In addition to Keay 25.2 the site produced also other varieties of Late Roman Amphorae, mainly Keay types 35, 55, 56, 57 and 62 A (Fantuzzi et al., 2015a,b and references therein).



1. [Download high-res image \(142KB\)](#)
2. [Download full-size image](#)

Fig. 2. Medium-sized cylindrical-shaped Keay 25.2 amphora ([Keay, 1984](#)).

### 3. Geological context

The site of Sidi Zahruni is located near the modern town of Beni Khiair, 6 km north-east of Nabeul, and covers an area of 13 ha between the Wadi El Sohil and the Jebel Al Qola, and crossed by the Wadi El Kebir ([Fig. 1](#)). It is at a short distance from the sea, from which it is separated by a system of dunes (recent and Marine Tyrrhenien) and outcrops of Late Pliocene sandstone. Sidi Zahruni is at the base of the southern side of the massif of Jebel Al Qola (75 m high), an anticline consisting of a stratigraphic succession of Tertiary sedimentary rock of marine origin, formed by few meter layers of grey-blue clays, alternating with layers of quartz-sandstone and rare layers of thinner limestone and marl. More in detail, the area surrounding the site is characterised, in addition to Quaternary deposits (soils, crusting limestone) by the presence of two geological formations: i) the Upper Tortonian-Lower Messinian Beni Khiair Formation, geologically defined near the village of Beni Khiair, close to Nabeul, and consisting of a 15m thick sequence of sandstone and clay, with some intercalations of limestone and marl; ii) the Messinian Oued El Kebir Formation, composed of sandstone, clay, sand, and small banks of limestone. The clay levels within these formations represent the possible clay source exploited during the Late Roman Times for the amphorae production.

### 4. Materials and methods

A set of 43 potsherds from Keay 25.2 amphorae (labelled CZ) were selected from the site and archaeometrically analysed. In particular, they were collected from the surface, since the site was not excavated up to now, and therefore it cannot be excluded that they may also represent ceramic wastes from the site production. In the area of the site various kilns have been identified. Most of potsherds have a fine-grained paste, reddish-orange to reddish-brown in colour. In some cases, the surface is grey; in others, both paste and surface (samples CZ-1-230, CZ-1-227, CZ-10-6, CZ-5-97) are grey, presumably due to a change in the firing atmosphere. The outermost portions of the amphorae are characterised by a white/cream colour, due to the effect of salt during firing, since salted sea water was used to mix the clay ([Sherriff et al., 2002a,b](#)).

Two clay samples (Clay1, Clay2) were collected from the undisturbed clay-rich layers of the nearby Upper Miocene deposits, at a depth of 30–40 cm. In detail, Clay1 comes from the Upper Tortonian-Lower Messinian Beni Khiair Formation, whereas Clay2 was collected from the late Messinian clayey deposit of the Oued El Kebir Formation ([Fig. 1b](#)). Both clays are suitable for ceramic manufacture, especially that from the Chabat Al Qola massif, although even nowadays it is exploited by a brick factory located near the archaeological site. Traces of clay exploitation in ancient times are still visible along the slopes of the massif.



All amphora fragments were thin-sectioned and petrographically analysed, and their ceramic fabrics were described following the procedure of [Whitbread \(1989, 1995\)](#). Samples were divided into petrographic groups and subgroups according to the type, abundance and grain-size of inclusions. One representative sample was selected for each subgroup and analysed by scanning electron microscopy (SEM) on a CamScan MX 2500 equipped with a LaB<sub>6</sub> cathode, coupled to an EDS spectrometer, and operating at 20 kV and 160 nA. For each sample, a set of about 120 back-scattered (SEM-BSE) images (resolution 1280 x 1024 pixel) were merged, covering almost the entire surface of the thin section (approximately 46 x 27 mm). The resulting image was processed with open source software (ImageJ 1.44p, National Institutes of Health, USA; MultiSpec 3.1, Purdue Research Foundation) to extract quantitative data of the textural features of the pottery paste, i.e., the abundance of its constituents (inclusions, voids, matrix) and the grain-size distribution of inclusions. Particle analysis of binary images gave the Minimum Feret diameter (MinFeret) of the grains, defined as the shortest distance between any two points along the selected grain boundary, corresponding to the minimum size of the inclusions. Particle grain-size were described according to the MinFeret diameter because it provides results similar to those obtained by sieving in sedimentological studies. The cut-off point between matrix inclusions and grains was set at 10 µm, according to [Whitbread \(1995\)](#). Image treatment followed the method of [Dal Sasso et al. \(2014\)](#).

The mineralogical composition of all samples was determined by X-ray powder diffraction (XRPD) on a Philips PW 3710 diffractometer in Bragg–Brentano geometry, equipped with a Cu X-ray tube, operating at 40 kV and 40 mA in the 4°–70° 2θ range, with a step-size of 0.02° and a counting time of 1 s per step. In order to obtain homogeneous groups with analogous mineralogical composition, cluster analysis of the whole dataset was performed with X'Pert HighScore Plus® software, according to the procedure of [Piovesan et al. \(2013\)](#) for analysis of mortars and of [Maritan et al. \(2015\)](#) for that of pottery.

Quantitative chemical analyses of major, minor (SiO<sub>2</sub>, TiO<sub>2</sub>, Al<sub>2</sub>O<sub>3</sub>, Fe<sub>2</sub>O<sub>3</sub>, MnO, MgO, CaO, Na<sub>2</sub>O, K<sub>2</sub>O, P<sub>2</sub>O<sub>5</sub>) and trace elements (Sc, V, Cr, Co, Ni, Cu, Zn, Ga, Rb, Sr, Y, Zr, Nb, Ba, La, Ce, Nd, Pb, Th, U) were performed on both potsherds and clay materials by X-ray fluorescence (XRF) on a Philips PW2400 spectrometer, in order to define the chemical variability of the potsherds and their compatibility with the petrographic subgroups and the local base-clays. Potsherds and clay specimens were reduced to powder in an agate mortar, after removal of the surface layer of potsherds to avoid any contamination, and then prepared as beads from calcined powder and Li<sub>2</sub>B<sub>4</sub>O<sub>7</sub>, dilution ratio 1:10. A set of geological standards, as analytically tested by the international scientific community ([Govindaraju, 1994](#)), was used for calibration; they were supplied by the following agencies: USGS (United States Geological Survey, Reston, USA), CRPG (Centre de Recherches Pétrographiques et Géochimiques, France), ANRT (Association Nationale de la Recherche Technique, Paris, France), GIT-IWG (Groupe International de Travail - International Working Group, France), RIAP (Research Institute of Applied Physics, Irkutsk, Russia), GSJ (Geological Survey of Japan, Japan), MINTEK (Council for Mineral Technology, South Africa) and WIHG (Wadia Institute of Himalayan Geology, India).

Chemical data were processed with standard statistical tools such as Principal Component Analysis (PCA) and cluster analysis (CA) with Statgraphics® Centurion XVI software. The R Project for Statistical Computing was used to explore the compositional variation matrix, according to the method of [Buxeda i Garrigós \(1999\)](#) to evaluate any contamination. Multivariate analyses were carried out on a subset of elements, excluding those with a low ratio between total variation (vt) and variance ( $\tau.i$ ). Raw data were standardised according to procedures designed by [Vitali and Franklin \(1986\)](#), [Baxter \(1999\)](#) and [Buxeda i Garrigós \(1999\)](#), by log-normal ratio transformation in order to avoid misclassifications due to the different orders of magnitude and range of variation of the variables ([Fermo et al., 2008](#)).

## 5. Results and discussion

### 5.1. Petrography

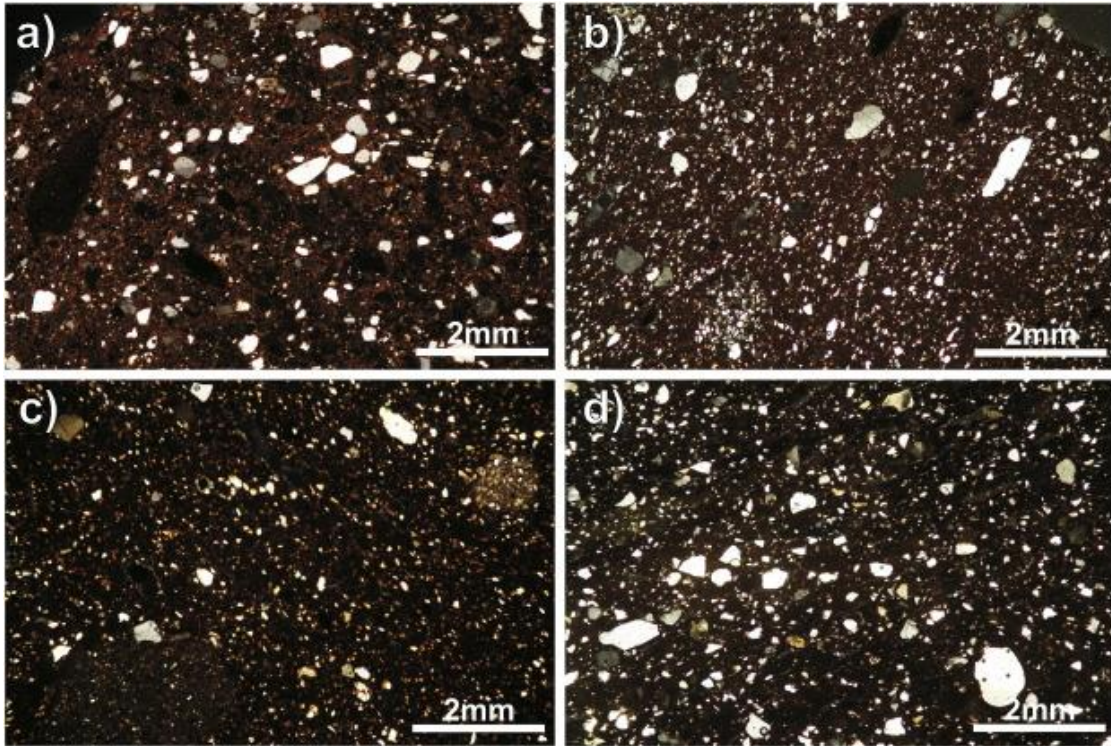
Petrographic analysis of thin sections facilitated the identification of three fabrics according to similarities and differences, especially in the nature, shape and arrangement of aplastic inclusions, voids and micromass.

- Petro-group 1: PG1

This group of 17 samples contained about 30% of very poorly sorted aplastic inclusions, displaying almost unimodal grain-size distribution. In some cases, medium sand-sized inclusions also occurred, showing a grain-size gap with respect to the smaller fraction. The inclusions were mainly fine to medium sand-sized quartz, occasionally associated with rare crystals of pyroxene, plagioclase and mica, small fragments of chert, micritic and sparitic limestone, sandstone, and microfossils. The pores were generally small to medium in size ( $< 1$  mm), occurring mainly as vesicles, but also as elongated subparallel channels and irregular-shaped vughs ([Fig. 3a](#)). The micromass was generally iron-rich, optically inactive.

- Petro-group 2: PG2





1. [Download high-res image \(2MB\)](#)
2. [Download full-size image](#)

Fig. 3. Photomicrographs of representative samples of the petrographic groups: a) PG1; b) PG2a; c) PG2b; d) PG3. Cross polars.

This group contained 22 samples, characterised by abundant very fine-grained inclusions ( $< 300 \mu\text{m}$ ), predominantly composed of angular quartz grains, and a coarser fraction of rare rounded (aeolian) grains of quartz and quartz-sandstone, usually with calcareous cement. Coarse fragments of fine quartz-sandstone and sub-angular to rounded quartz grains were occasionally found. As regards inclusion composition, the samples of this group were similar to those of PG1, but had smaller quartz grains, with bimodal grain-size distribution. Rare fragments of microfossils and iron-rich inclusions were also found in some potsherds. Two distinct subgroups were distinguished: one with higher (PG2a) and one with lower (PG2b) percentages of silt and fine sand-sized inclusions (Fig. 3b,c).

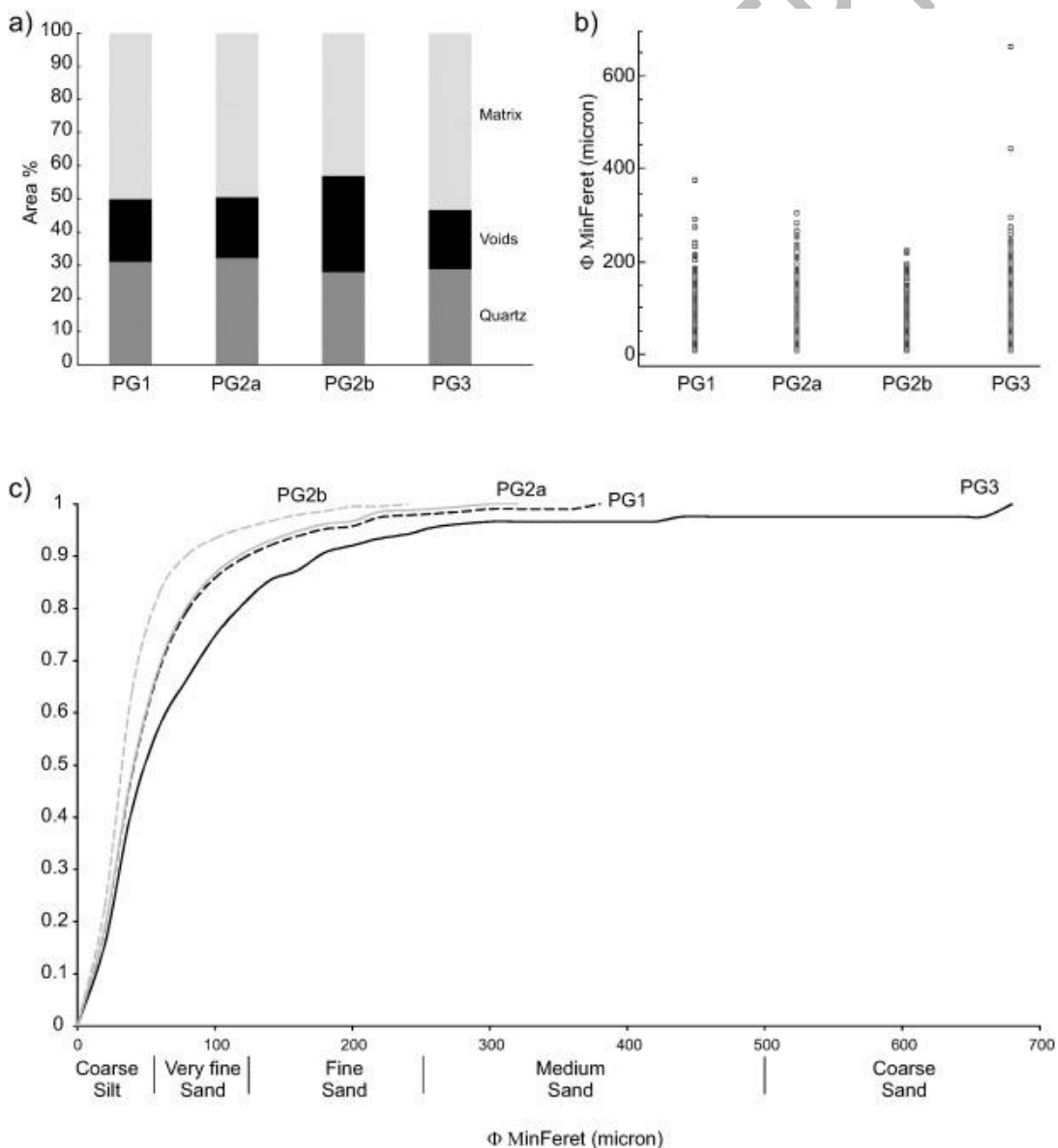
- Petro-group 3: PG3

This was a small group of only four samples, characterised by moderately sorted mainly medium-sized inclusions, with unimodal grain-size distribution, composed mainly of sub-angular to sub-rounded quartz, with rare coarser aeolian quartz grains, up to  $700 \mu\text{m}$ . Compared with PG1 and PG2, the silt and fine sand-sized fraction were lower, and the abundance of coarse sand higher. The groundmass was moderately to very porous, dark reddish-brown in colour, and optically inactive. A few crystals of plagioclase, biotite, pyroxene, opaque minerals chert and quartz-sandstone were also found (Fig. 3d).

The presence of siltstone and sandstone fragments in most of the amphorae was consistent with the clayey materials from the Upper Miocene deposits (Chabat Al Qola massif), which were also rich in sandstone grains.

As the petrographic groups were distinguished mainly according to their grain-size distribution, some representative samples of each petro-group were subjected to digital image analysis (DIA) on scanning electron microscope back-scattered (SEM-BSE) images, to quantify these differences.

The DIA results showed that all the above petro-groups had similar c:f:v (coarse:fine:voids) ratios, as clearly revealed by the histograms of their percentages (Fig. 4a), although their grain-size distribution of inclusions differed (Fig. 4b,c). In more detail, groups PG1 and PG2a appeared to be very similar, although the former was richer in medium sand-sized inclusions. Petro-group PG2b had the lowest percentages of medium and coarse inclusions, whereas petro-group PG3 has the highest ones.

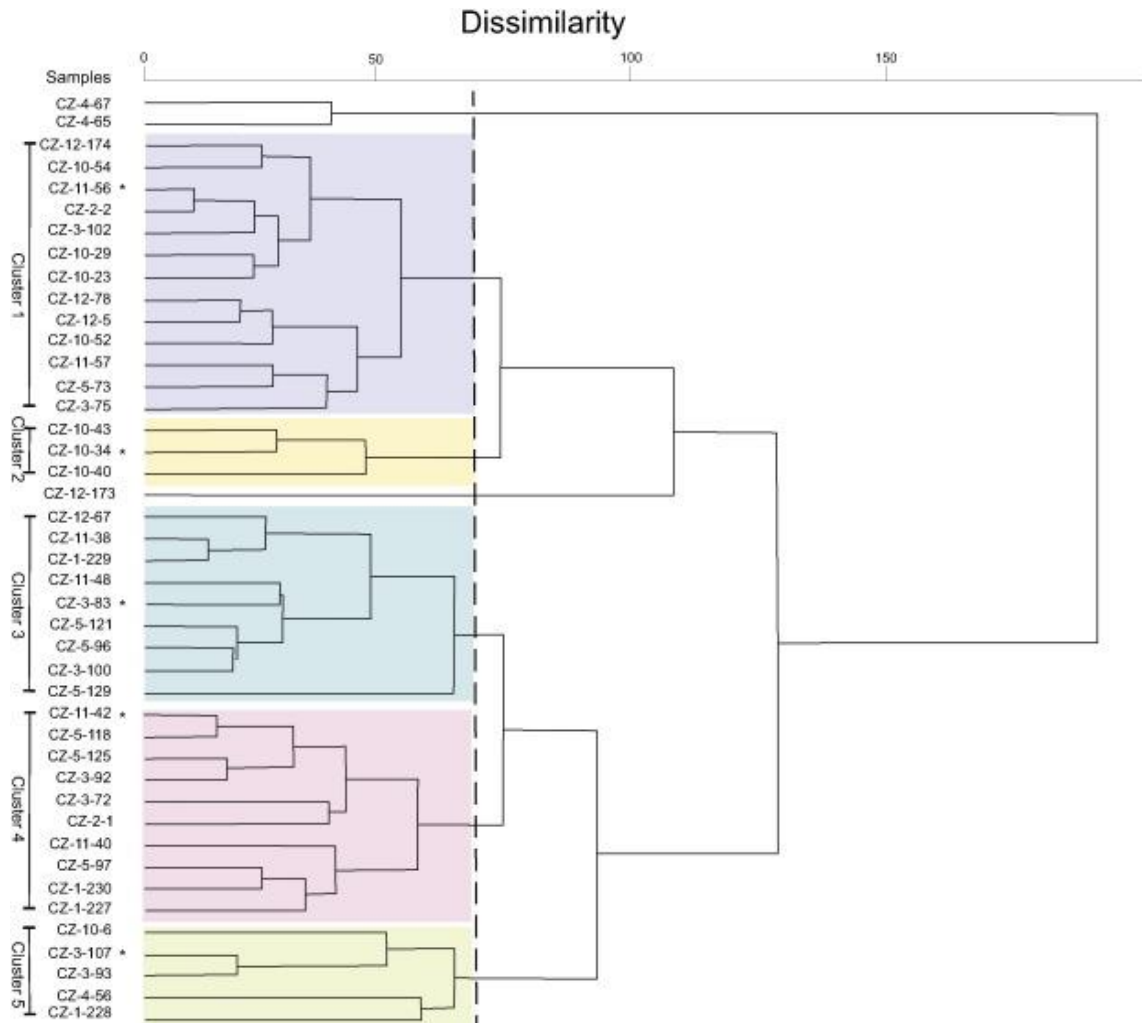


1. [Download high-res image \(385KB\)](#)
2. [Download full-size image](#)

Fig. 4. a) Histogram of quartz, voids and matrix percentage; b) dispersion diagram of quartz inclusions; c) cumulative grain-size curves of inclusions, as obtained from DIA, for samples representative of the various petrographic groups.

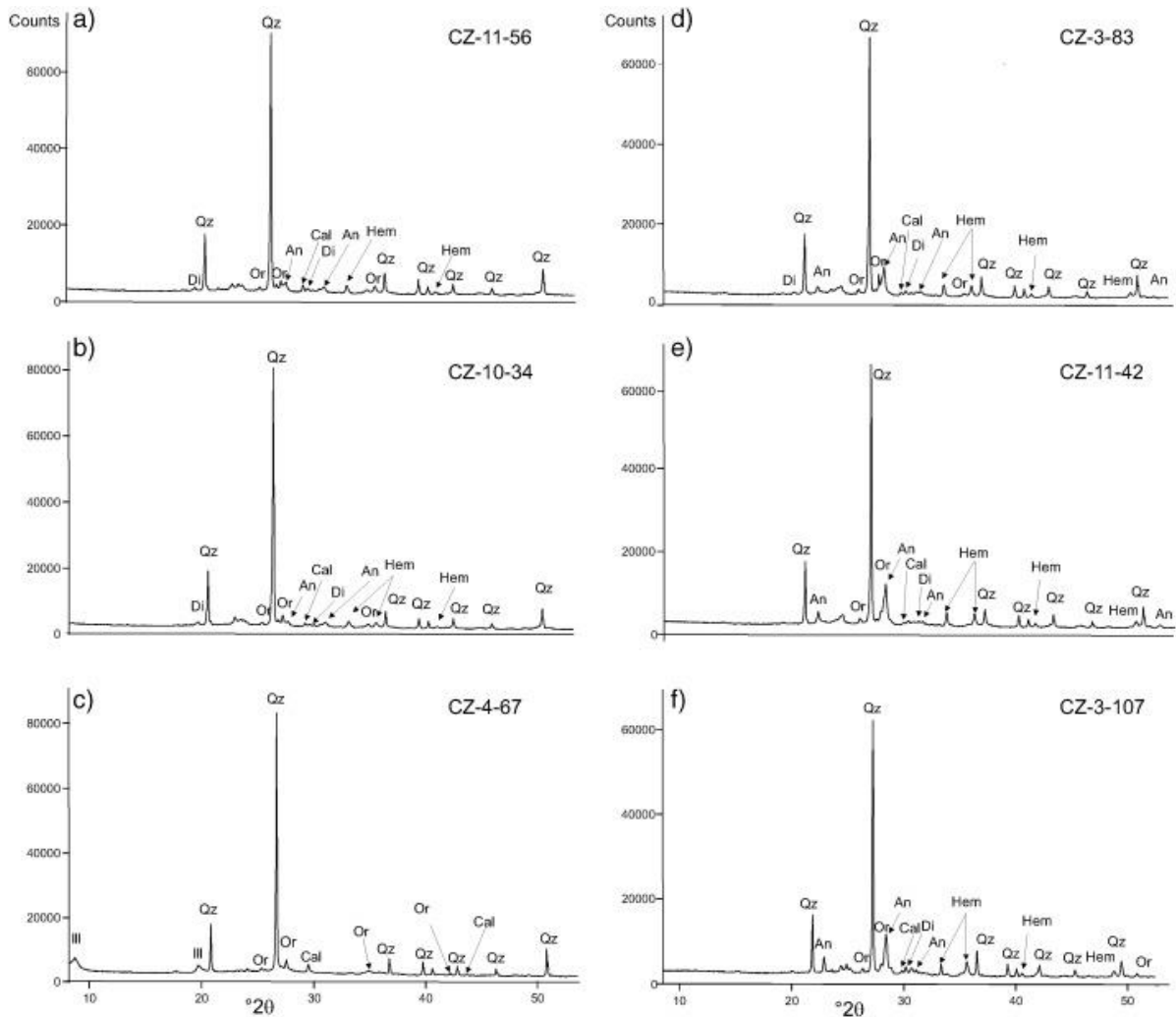
## 5.2. Mineralogical composition and firing temperature

As regards the mineralogical composition, the cluster analysis of XRPD patterns (Fig. 5) showed that the samples fell into five clusters, with the exception of three sherds (outliers: CZ-4-65, CZ-4-67 and CZ-12-173). The diffraction patterns of the most representative sample of each cluster showed the same mineralogical association of quartz, orthoclase, calcite, anorthite, hematite and diopside; therefore, the clusters differed in their relative abundances of mineral phases. The resulting dendrogram showed that the sherds of clusters 1 and 2 were very similar, due to the presence of calcite and the low anorthite content (Fig. 6a,b), whereas those of clusters 3, 4 and 5 (Fig. 6d,e,f) shared a higher proportion of anorthite. The three isolated samples were composed of quartz, orthoclase, illite and calcite (Fig. 6c), in addition to a relatively small amount of hematite in sample CZ-12-173. The mineralogical similarities between clusters indicated that quartz-rich and moderate-poor carbonate clayey materials were used to produce these amphorae. The small differences in the relative proportions of the mineral phases may have been due to firing conditions (maximum firing temperature and atmosphere) and perhaps on the addition of a temper.



1. [Download high-res image \(349KB\)](#)
2. [Download full-size image](#)

Fig. 5. Dendrogram from cluster analysis of XRPD patterns of Keay 25.2 amphorae from Sidi Zahruni site, according to Euclidean distance and average linkage method on position and intensity of peaks. \*: most representative samples within each cluster.



1. [Download high-res image \(497KB\)](#)
2. [Download full-size image](#)

Fig. 6. XRPD patterns of most representative sample (sample name: top right of each pattern) for each cluster identified in the dendrogram of Fig. 6. Abbreviations: Qz: quartz, Ill: illite, Mi: microcline, Or: orthoclase, Cal: calcite, Hem: hematite, Di: diopside, An: anorthite ([Whitney and Evans, 2010](#)).

XRPD analysis provided the key to reconstruction of firing temperatures according to mineralogical changes during firing ([Maritan et al., 2005, 2006; Nodari et al., 2007; Grifa et al., 2009](#)). Regarding outliers, in which some calcite and illite were detected and newly formed minerals were not identified, the firing temperature was 800–850 °C. According to their optically active groundmass in thin section ([Fig. 3a](#)), these samples were relatively low-fired products. In the potsherds of clusters 1 and 2, anorthite and diopside became detectable in the diffraction patterns and calcite was still present in trace amounts, indicating relatively higher firing temperatures, around 850–900 °C. In these samples, also amorphous phase can be recognised, as the background is quite high, especially in the region between 20° and 30° 2θ. The majority of samples (clusters 3, 4, 5) had higher quantities of anorthite and diopside, suggesting firing higher than 900 °C but lower than 1000 °C, since mullite, which would be expected to form after the decomposition of phyllosilicates ([Gualtieri et al., 1995; Cultrone et al., 2004](#)), lacks.



XRPD analysis of the two clay samples (Clay 1 and Clay 2), collected near Sidi Zahrani, showed remarkable similarities in their mineralogical compositions, since they were both composed mainly of quartz, calcite and K-feldspar, in addition to clay minerals, illite and kaolinite. Clay1 had a notably higher content of calcite.

### 5.3. Chemical composition and raw material provenance

The chemical composition of the amphorae was quite homogeneous, although small differences were observed for some elements (Table 1). More in detail, the amphorae are calcareous, although not highly, have a relatively high content of iron, which determine their reddish-brown colour, and of silica due also the nature of their inclusions (mainly quartz), whereas alumina is relatively low (Table 1). The statistical treatment of the chemical data, according to cluster analysis (performed on 26 elements and excluding Sc, U, Sr and CaO due to their high  $\tau$  values: 19.539, 15.222, 4.787 and 4.618, respectively), shows that the amphorae tended to cluster into two main groups, with the exception of a few samples (CZ-3-93, CZ-4-67, CZ-2-2, CZ-10-6 and CZ-11-40) and the two clays (Clay1 and Clay2), which show a high dissimilarity level (Fig. 7). Most of the potsherds of PG1 tended to group in cluster CL2, separately from those of PG2 and PG3, which clustered in CL1. This was also confirmed by the PCA score plot (Fig. 8), in which almost all the PG1 potsherds had negative values of PC1 and were richer in MgO and Ni, whereas those of PG2 and PG3 mainly had positive values of PC1 and were richer in SiO<sub>2</sub>, TiO<sub>2</sub>, K<sub>2</sub>O, Fe<sub>2</sub>O<sub>3</sub> and trace elements such as Ce, Nb, Ba, Zn, Cu, Rb, Zr, Y and Th. As regards clay materials, the two samples were isolated from the potsherds, but Clay2 was closer to the amphorae cloud, whereas Clay1 was chemically different from all the samples because of its high CaO concentration (Table 1). Although many archaeometric studies based on petrographic analysis have been carried out in recent years on Late Roman African amphorae from various workshops in Tunisia and found in many consumption sites in the Mediterranean area (Sherriff et al., 2002a,b; Capelli, 2005; Capelli and Leitch, 2011; Fantuzzi et al., 2015a,b and references therein), only very few African amphorae have been chemically analysed (Sherriff et al., 2002a,b; Fantuzzi et al., 2015a,b). Statistical analysis of these data with those produced in the present research shows a clear distinction between the amphorae produced at Sidi Zahrani and those found in Catalonia attributed to various workshops in the Nabeul area (Sidi Zahrani, Labayedh, Choggafia) and central Tunisia (Moknine and Henchir Chekaf) (Fig. 9). In more detail, the amphorae found in Tarragona (Catalonia, Spain) (Sidi Zahrani in Fig. 9), previously defined by Fantuzzi et al. (2015a) as produced at Sidi Zahrani on the basis of typology (Key 35 A, Key 35B, Key 27, Spatheion 1) and petrographic features, do not cluster with those of Sidi Zahrani due to their higher contents of Ce and Nb (Fig. 10). Despite they are compositionally more similar to those of the central Tunisian workshop of Henchir Chekaf, it cannot be excluded that the geochemical differences with the samples collected at Sidi Zahrani are due to the different instrument used to perform the analysis or to the fact that those analysed by Fantuzzi et al. (2015a) come from a consumption site. In addition, the amphorae of Labayedh and Moknine are geochemically different from those of Sidi Zahrani (Nabeul) and Henchir Chekaf (central Tunisia), since they have higher contents of Nb, Ce and Cr (Fig. 10), whereas the amphorae of Choggafia are geochemically different from all the others due to their higher Zr content. Lastly, three amphorae



from Sidi Zahrani (CZ-4-67, CZ-11-40, CZ-2-2) exhibit a higher dissimilarity level (Fig. 9) with respect to the other amphorae analysed, due to their lower Na<sub>2</sub>O and Pb contents in the former two and higher Ni concentration in the latter (Fig. 10).

Table 1. Geochemical composition by XRF of analysed samples (ceramic and clays) with the literature data for amphorae attributed to *Sidi Zahrani* (in italic) (Fantuzzi et al., 2015a) and other sites of the Nabeul area (Fantuzzi et al., 2015b). Major and minor elements expressed as wt% of oxides, trace elements as ppm. Petrographic group for samples of Sidi Zahrani is also reported.

| Sampl es          | Pet ro-gro up | Si O <sub>2</sub> | Ti O <sub>2</sub> | Al <sub>2</sub> O <sub>3</sub> | Fe <sub>2</sub> O <sub>3</sub> | Mn O  | Mg O  | Ca O  | Na <sub>2</sub> O | K <sub>2</sub> O | P <sub>2</sub> O <sub>5</sub> | T ot   | L. O ·I | S c  | V    | C r  | C o  | N i  | C u  | Z n  | G a | R b  | S r | Y    | Z r | N b  | B a | L a | C e | N d | P b | T h | U |
|-------------------|---------------|-------------------|-------------------|--------------------------------|--------------------------------|-------|-------|-------|-------------------|------------------|-------------------------------|--------|---------|------|------|------|------|------|------|------|-----|------|-----|------|-----|------|-----|-----|-----|-----|-----|-----|---|
| Potsherds. n = 43 |               |                   |                   |                                |                                |       |       |       |                   |                  |                               |        |         |      |      |      |      |      |      |      |     |      |     |      |     |      |     |     |     |     |     |     |   |
| <i>CZ-1-227</i>   | PG2           | 69.02             | 0.087             | 1.442                          | 5.735                          | 0.093 | 1.415 | 4.162 | 0.698             | 2.195            | 0.992                         | 99.46  | 1.13    | 1.15 | 1.02 | 1.07 | 2.29 | 2.29 | 1.03 | 2.23 | 9.8 | 2.17 | 3.0 | 3.68 | 1.8 | 4.34 | 4.1 | 7.8 | 3.4 | 2.4 | 9   | 3   |   |
| <i>CZ-1-228</i>   | PG1           | 66.35             | 0.087             | 1.539                          | 6.34                           | 0.063 | 2.65  | 4.79  | 0.82              | 2.60             | 0.998                         | 99.0   | 1.02    | 1.32 | 1.13 | 1.18 | 3.2  | 1.9  | 1.04 | 2.6  | 9.4 | 2.54 | 2.9 | 2.57 | 1.9 | 3.21 | 4.9 | 6.9 | 3.9 | 2.3 | 9   | 7   |   |
| <i>CZ-1-230</i>   | PG1           | 65.41             | 0.088             | 1.57                           | 6.36                           | 0.073 | 2.79  | 5.04  | 0.80              | 2.82             | 1.04                          | 100.87 | 0.91    | 1.21 | 1.16 | 1.32 | 2.8  | 2.11 | 1.1  | 2.8  | 9.8 | 2.71 | 2.9 | 2.55 | 2.0 | 3.30 | 5.1 | 8.0 | 4.6 | 2.4 | 1.2 | 4   |   |
| <i>CZ-1-229</i>   | PG2           | 66.77             | 0.085             | 1.42                           | 5.71                           | 0.023 | 2.33  | 6.79  | 0.83              | 2.83             | 0.994                         | 99.73  | 1.02    | 1.10 | 1.00 | 1.07 | 2.8  | 2.9  | 1.03 | 2.4  | 9.2 | 2.98 | 3.0 | 3.64 | 1.7 | 4.43 | 4.7 | 6.7 | 3.6 | 2.4 | 1.1 | 5   |   |
| <i>CZ-2-1</i>     | PG2           | 65.05             | 0.089             | 1.505                          | 6.20                           | 0.023 | 2.15  | 7.10  | 0.73              | 2.66             | 0.913                         | 100.92 | 0.92    | 1.17 | 1.10 | 1.19 | 3.5  | 2.7  | 1.04 | 2.5  | 9.8 | 2.63 | 3.1 | 3.43 | 2.0 | 3.34 | 3.4 | 8.1 | 3.6 | 2.2 | 1.3 | 1   |   |
| <i>CZ-2-2</i>     | PG1           | 67.52             | 0.081             | 1.431                          | 6.22                           | 0.054 | 2.51  | 5.14  | 0.58              | 2.81             | 0.914                         | 100.81 | 1.11    | 1.19 | 1.04 | 1.06 | 6.8  | 2.7  | 1.04 | 2.4  | 9.6 | 3.68 | 2.8 | 2.77 | 1.6 | 3.22 | 3.4 | 6.7 | 3.6 | 3.6 | 7   | 6   |   |

| Sa<br>m<br>pl<br>es | Pet<br>ro<br>gro<br>up | Si<br>O <sub>2</sub> | Ti<br>O <sub>3</sub> | Al <sub>2</sub> O <sub>3</sub> | Fe <sub>2</sub> O <sub>3</sub> | MnO  | MgO  | CaO  | Na <sub>2</sub> O | K <sub>2</sub> O | P <sub>2</sub> O <sub>5</sub> | Tot    | L.O-I | Sc   | V    | Cr  | Co  | Ni  | Cu   | Zn  | Ga   | Rb   | Sr   | Y    | Zr   | Nb   | Ba   | La  | Ce  | Nd  | Pb  | Th  | U |
|---------------------|------------------------|----------------------|----------------------|--------------------------------|--------------------------------|------|------|------|-------------------|------------------|-------------------------------|--------|-------|------|------|-----|-----|-----|------|-----|------|------|------|------|------|------|------|-----|-----|-----|-----|-----|---|
| CZ-3-72             | PG1                    | 64.38                | 0.88                 | 15.84                          | 6.58                           | 0.06 | 2.41 | 6.06 | 0.49              | 2.58             | 0.17                          | 99.45  | 1.23  | 1.33 | 1.22 | 1.9 | 4.0 | 2.6 | 1.09 | 2.8 | 9.5  | 4.35 | 2.7  | 2.38 | 1.8  | 3.55 | 4.8  | 7.7 | 4.2 | 2.2 | 1.1 | 7   |   |
| CZ-3-75             | PG1                    | 64.61                | 0.89                 | 15.59                          | 6.23                           | 0.04 | 3.20 | 5.80 | 0.63              | 2.73             | 0.13                          | 99.85  | 1.42  | 1.32 | 1.10 | 1.5 | 3.3 | 3.0 | 1.07 | 2.6 | 1.04 | 6.34 | 3.1  | 3.06 | 1.9  | 3.36 | 3.1  | 6.7 | 4.6 | 2.9 | 7   | 4   |   |
| CZ-3-83             | PG1                    | 66.56                | 0.87                 | 15.15                          | 6.43                           | 0.23 | 2.37 | 5.37 | 0.62              | 2.68             | 0.13                          | 100.10 | 1.14  | 1.23 | 1.08 | 1.7 | 3.3 | 2.8 | 1.04 | 2.4 | 9.8  | 2.50 | 3.0  | 3.01 | 1.9  | 3.54 | 4.2  | 6.7 | 3.5 | 2.6 | 1.1 | 1   |   |
| CZ-3-92             | PG2                    | 65.72                | 0.91                 | 15.61                          | 6.48                           | 0.03 | 2.12 | 4.70 | 0.62              | 2.89             | 0.16                          | 99.24  | 1.17  | 1.25 | 1.11 | 1.8 | 3.1 | 2.7 | 1.11 | 2.6 | 9.7  | 2.45 | 3.1  | 3.08 | 1.8  | 4.00 | 4.6  | 7.4 | 4.5 | 2.4 | 1.1 | 5   |   |
| CZ-3-93             | PG2                    | 70.39                | 0.81                 | 12.41                          | 4.93                           | 0.16 | 1.61 | 5.61 | 0.66              | 2.51             | 0.11                          | 99.10  | 1.22  | 1.03 | 0.9  | 1.2 | 2.4 | 2.2 | 0.8  | 2.2 | 2.2  | 7.9  | 2.04 | 2.9  | 4.08 | 1.7  | 3.63 | 2.0 | 6.5 | 3.8 | 2.6 | 1.0 | 1 |
| CZ-3-100            | PG2                    | 67.83                | 0.88                 | 14.55                          | 5.78                           | 0.03 | 2.05 | 4.95 | 0.52              | 2.72             | 0.15                          | 99.42  | 1.56  | 1.15 | 1.06 | 1.7 | 2.9 | 3.0 | 1.04 | 2.5 | 9.5  | 2.29 | 3.2  | 3.56 | 1.9  | 4.23 | 3.5  | 6.7 | 3.9 | 2.8 | 1.2 | 4   |   |
| CZ-3-102            | PG2                    | 66.61                | 0.94                 | 14.98                          | 5.93                           | 0.04 | 2.04 | 6.00 | 0.56              | 2.78             | 0.15                          | 99.86  | 1.95  | 1.19 | 1.05 | 1.7 | 3.1 | 3.1 | 1.04 | 2.4 | 1.02 | 2.60 | 3.3  | 3.65 | 1.9  | 4.03 | 5.4  | 7.1 | 4.0 | 2.4 | 1.2 | 1   |   |
| CZ-3-107            | PG3                    | 68.31                | 0.82                 | 12.97                          | 5.60                           | 0.09 | 1.96 | 6.57 | 0.62              | 2.40             | 0.14                          | 99.43  | 1.02  | 1.10 | 0.98 | 1.6 | 2.6 | 2.3 | 0.92 | 2.1 | 8.4  | 6.57 | 2.7  | 3.84 | 1.6  | 3.42 | 2.9  | 6.6 | 4.2 | 2.3 | 7   | 7   |   |
| CZ-4-56             | PG2                    | 70.03                | 0.85                 | 13.95                          | 5.56                           | 0.03 | 2.00 | 3.67 | 0.75              | 2.71             | 0.14                          | 99.69  | 1.27  | 1.18 | 0.98 | 1.8 | 2.7 | 2.2 | 1.00 | 2.4 | 9.4  | 3.20 | 3.1  | 3.45 | 1.8  | 3.44 | 3.8  | 6.5 | 3.7 | 2.4 | 1.0 | 6   |   |

| Sampl<br>es | Pet<br>ro-<br>grop<br>up | Si<br>O <sub>2</sub> | Ti<br>O <sub>3</sub> | Al <sub>2</sub><br>O <sub>3</sub> | Fe <sub>2</sub><br>O <sub>3</sub> | Mn<br>O | Mg<br>O | Ca<br>O | Na <sub>2</sub><br>O | K <sub>2</sub><br>O | P <sub>2</sub><br>O <sub>5</sub> | Tot<br>al | Sc   | V    | Cr   | Co  | Ni  | Cu  | Zn   | Ga  | Rb   | Sr   | Y   | Zr   | Nb  | Ba   | La  | Ce  | Pr  | Tb  | U   |   |
|-------------|--------------------------|----------------------|----------------------|-----------------------------------|-----------------------------------|---------|---------|---------|----------------------|---------------------|----------------------------------|-----------|------|------|------|-----|-----|-----|------|-----|------|------|-----|------|-----|------|-----|-----|-----|-----|-----|---|
| CZ-4-65     | PG1                      | 70.22                | 0.87                 | 15.64                             | 5.90                              | 0.23    | 2.27    | 1.32    | 0.57                 | 3.03                | 0.14                             | 99.99     | 3.33 | 12.6 | 10.4 | 1.6 | 3.2 | 3.4 | 10.8 | 2.6 | 10.3 | 2.80 | 3.3 | 29.3 | 1.8 | 44.9 | 4.1 | 7.7 | 3.7 | 2.2 | 1.3 | 6 |
| CZ-4-67     | PG1                      | 65.62                | 0.88                 | 15.81                             | 6.51                              | 0.44    | 2.48    | 5.18    | 0.37                 | 2.87                | 0.21                             | 99.97     | 6.08 | 12.8 | 10.8 | 1.7 | 3.8 | 3.8 | 11.1 | 2.7 | 8.4  | 4.37 | 3.0 | 26.5 | 1.8 | 51.4 | 4.9 | 6.9 | 2.8 | 2.7 | 9   | 4 |
| CZ-5-73     | PG2                      | 68.23                | 0.81                 | 13.37                             | 5.29                              | 0.33    | 2.30    | 6.50    | 0.76                 | 2.60                | 0.13                             | 100.05    | 1.52 | 10.3 | 9.2  | 1.5 | 2.6 | 3.2 | 10.3 | 2.3 | 9.2  | 3.12 | 2.9 | 35.4 | 1.6 | 36.7 | 4.1 | 6.8 | 3.2 | 2.3 | 1.1 | 4 |
| CZ-5-96     | PG1                      | 66.21                | 0.84                 | 14.96                             | 6.57                              | 0.45    | 4.25    | 0.61    | 0.96                 | 2.96                | 0.14                             | 99.43     | 1.46 | 11.9 | 10.7 | 1.4 | 3.3 | 2.9 | 10.2 | 2.6 | 9.9  | 6.50 | 2.7 | 26.5 | 1.6 | 33.0 | 4.3 | 7.5 | 4.0 | 2.1 | 8   | 8 |
| CZ-5-97     | PG2                      | 66.70                | 0.91                 | 15.47                             | 6.16                              | 0.37    | 4.09    | 0.61    | 0.91                 | 2.92                | 0.15                             | 100.00    | 0.74 | 13.1 | 11.0 | 1.5 | 3.3 | 2.7 | 10.7 | 2.7 | 10.0 | 2.34 | 3.1 | 34.8 | 1.9 | 36.5 | 4.9 | 7.4 | 3.9 | 2.5 | 1.1 | 3 |
| CZ-5-121    | PG3                      | 65.85                | 0.89                 | 15.09                             | 6.09                              | 0.49    | 4.84    | 0.61    | 0.91                 | 3.01                | 0.15                             | 99.52     | 1.78 | 12.3 | 11.1 | 1.5 | 3.6 | 2.8 | 10.7 | 2.6 | 9.6  | 5.99 | 2.8 | 24.5 | 1.6 | 33.9 | 3.3 | 6.8 | 5.0 | 2.8 | 7   | 5 |
| CZ-5-125    | PG1                      | 65.78                | 0.90                 | 15.82                             | 6.40                              | 0.38    | 4.35    | 0.69    | 0.99                 | 2.69                | 0.11                             | 99.35     | 1.36 | 12.8 | 11.5 | 1.8 | 3.2 | 2.0 | 10.3 | 2.7 | 9.5  | 3.08 | 3.0 | 28.5 | 1.8 | 33.9 | 3.5 | 8.0 | 4.3 | 1.8 | 1.5 | 8 |
| CZ-5-129    | PG2                      | 66.36                | 0.96                 | 16.74                             | 6.64                              | 0.33    | 3.38    | 0.53    | 0.93                 | 2.97                | 0.17                             | 100.01    | 1.20 | 14.0 | 11.9 | 2.1 | 3.4 | 2.9 | 11.9 | 2.7 | 11.3 | 2.11 | 3.3 | 31.1 | 2.1 | 33.4 | 5.1 | 8.2 | 5.2 | 2.8 | 1.2 | 3 |
| CZ-10       | PG2                      | 64.68                | 0.84                 | 14.2                              | 7.00                              | 0.20    | 2.70    | 0.60    | 0.6                  | 2.6                 | 0.1                              | 99.9      | 0.8  | 12   | 10   | 1.9 | 3.1 | 2.9 | 11   | 2.3 | 8.9  | 9.1  | 3.1 | 35   | 1.8 | 37   | 3.7 | 6.4 | 3.3 | 2.5 | 3   | 3 |

| Sa<br>m<br>pl<br>es      | Pet<br>ro<br>gro<br>up | Si<br>O <sub>2</sub> | Ti<br>O <sub>2</sub> | Al <sub>2</sub><br>O <sub>3</sub> | Fe <sub>2</sub><br>O <sub>3</sub> | Mn<br>O      | Mg<br>O      | Ca<br>O      | Na <sub>2</sub><br>O | K <sub>2</sub><br>O | P <sub>2</sub><br>O <sub>5</sub> | Tot               | L<br>O <sub>1</sub> | S<br>c      | V           | Cr          | Co     | Ni     | Cu     | Zn          | Ga     | Rb          | Sr          | Y           | Zr          | Nb     | Ba          | La     | Ce     | Nd     | Pb     | Th     | U |  |
|--------------------------|------------------------|----------------------|----------------------|-----------------------------------|-----------------------------------|--------------|--------------|--------------|----------------------|---------------------|----------------------------------|-------------------|---------------------|-------------|-------------|-------------|--------|--------|--------|-------------|--------|-------------|-------------|-------------|-------------|--------|-------------|--------|--------|--------|--------|--------|---|--|
| -6                       |                        | 7                    | 5                    | 9                                 | 5                                 | 5            | 9            | 7            | 8                    | 5                   | 4                                | 4                 | 2                   | 3           | 1           |             |        |        |        | 8           |        |             | 5           |             | 4           |        | 9           |        |        |        |        |        |   |  |
| CZ<br>-<br>10<br>-<br>23 | PG<br>2                | 6<br>7.<br>8<br>5    | 0<br>9<br>9<br>0     | 1<br>4.<br>7<br>8                 | 5.<br>9<br>6                      | 0.<br>0<br>3 | 2.<br>0<br>7 | 4.<br>8<br>2 | 0.<br>5<br>1         | 2.<br>7<br>8        | 0.<br>1<br>5                     | 9<br>9.<br>8<br>5 | 2.<br>0<br>1        | 5           | 1<br>1<br>7 | 9<br>8      | 1<br>8 | 3<br>1 | 2<br>7 | 1<br>0<br>3 | 2<br>6 | 1<br>0<br>0 | 2<br>5<br>3 | 3<br>2      | 3<br>7<br>8 | 1<br>9 | 5<br>3<br>0 | 3<br>3 | 8<br>4 | 3<br>1 | 2<br>2 | 1<br>2 | 1 |  |
| CZ<br>-<br>10<br>-<br>29 | PG<br>1                | 6<br>9.<br>1<br>1    | 0<br>8<br>2<br>0     | 1<br>4.<br>0<br>0                 | 5.<br>6<br>0                      | 0.<br>0<br>3 | 1.<br>9<br>4 | 5.<br>2<br>3 | 0.<br>4<br>4         | 2.<br>4<br>7        | 0.<br>1<br>5                     | 9<br>9.<br>7<br>9 | 1.<br>6<br>2        | 7           | 1<br>1<br>5 | 9<br>7      | 1<br>4 | 2<br>9 | 2<br>9 | 1<br>0<br>0 | 2<br>4 | 9<br>4      | 2<br>4<br>6 | 2<br>9<br>3 | 2<br>9<br>3 | 1<br>7 | 3<br>6<br>9 | 3<br>0 | 6<br>6 | 4<br>1 | 2<br>7 | 1<br>2 | 4 |  |
| CZ<br>-<br>10<br>-<br>34 | PG<br>2                | 6<br>6.<br>8<br>4    | 0<br>9<br>2<br>3     | 1<br>5.<br>4<br>3                 | 6.<br>1<br>4                      | 0.<br>0<br>3 | 2.<br>0<br>9 | 4.<br>6<br>1 | 0.<br>5<br>9         | 2.<br>9<br>8        | 0.<br>1<br>6                     | 9<br>9.<br>7<br>9 | 1.<br>3<br>8        | 9           | 1<br>3<br>1 | 1<br>0<br>6 | 1<br>6 | 3<br>2 | 3<br>1 | 1<br>0<br>6 | 2<br>5 | 1<br>0<br>6 | 2<br>4<br>7 | 3<br>3<br>3 | 3<br>6<br>5 | 1<br>9 | 4<br>3<br>0 | 4<br>1 | 7<br>3 | 4<br>0 | 2<br>3 | 1<br>2 | 6 |  |
| CZ<br>-<br>10<br>-<br>40 | PG<br>2                | 6<br>7.<br>5<br>7    | 0<br>8<br>9<br>9     | 1<br>4.<br>2<br>9                 | 5.<br>9<br>2                      | 0.<br>0<br>3 | 2.<br>0<br>4 | 5.<br>6<br>8 | 0.<br>5<br>1         | 2.<br>7<br>0        | 0.<br>1<br>4                     | 9<br>9.<br>7<br>7 | 2.<br>9<br>3        | 1<br>1<br>0 | 1<br>0<br>0 | 1<br>7      | 2<br>9 | 3<br>3 | 3<br>3 | 1<br>0<br>2 | 2<br>4 | 9<br>9      | 2<br>5<br>7 | 3<br>2      | 4<br>0<br>7 | 1<br>8 | 5<br>1<br>0 | 3<br>3 | 7<br>2 | 3<br>4 | 2<br>4 | 1<br>0 | 1 |  |
| CZ<br>-<br>10<br>-<br>43 | PG<br>2                | 6<br>9.<br>5<br>8    | 0<br>8<br>2<br>3     | 1<br>2.<br>5<br>3                 | 5.<br>5<br>2                      | 0.<br>0<br>3 | 1.<br>8<br>0 | 6.<br>1<br>0 | 0.<br>5<br>6         | 2.<br>4<br>1        | 0.<br>1<br>4                     | 9<br>9.<br>4<br>9 | 1.<br>9<br>5        | 2           | 1<br>0<br>2 | 8<br>5      | 1<br>6 | 2<br>6 | 2<br>7 | 9<br>3      | 2<br>2 | 8<br>6      | 2<br>4<br>2 | 3<br>0      | 3<br>5<br>6 | 1<br>6 | 4<br>3<br>9 | 2<br>3 | 7<br>2 | 2<br>1 | 2<br>2 | 1<br>2 | 9 |  |
| CZ<br>-<br>10<br>-<br>52 | PG<br>2                | 6<br>7.<br>5<br>3    | 0<br>7<br>9          | 1<br>2.<br>8<br>9                 | 5.<br>4<br>1                      | 0.<br>0<br>5 | 2.<br>4<br>6 | 7.<br>7<br>4 | 0.<br>5<br>5         | 2.<br>5<br>4        | 0.<br>1<br>0                     | 1<br>0.<br>1<br>0 | 3.<br>4<br>9        | 2           | 9<br>9      | 9<br>1      | 1<br>6 | 2<br>6 | 3<br>1 | 9<br>3      | 2<br>2 | 8<br>8      | 3<br>7<br>6 | 2<br>8      | 3<br>1<br>9 | 1<br>7 | 5<br>0<br>2 | 3<br>0 | 7<br>1 | 3<br>1 | 2<br>3 | 8      | 1 |  |
| CZ<br>-<br>10<br>-<br>54 | PG<br>2                | 6<br>5.<br>9<br>9    | 0<br>9<br>9<br>3     | 1<br>5.<br>5<br>3                 | 6.<br>5<br>8                      | 0.<br>0<br>3 | 2.<br>1<br>6 | 4.<br>6<br>4 | 0.<br>4<br>8         | 2.<br>7<br>7        | 0.<br>1<br>5                     | 9<br>9.<br>2<br>6 | 1.<br>5<br>8        | 1<br>2      | 1<br>3<br>2 | 1<br>1<br>2 | 1<br>9 | 3<br>3 | 3<br>2 | 1<br>0<br>7 | 2<br>6 | 1<br>0<br>0 | 2<br>1<br>7 | 3<br>1      | 3<br>4<br>7 | 1<br>8 | 3<br>8<br>7 | 4<br>1 | 6<br>9 | 4<br>1 | 3<br>3 | 9      | 7 |  |
| CZ<br>-                  | PG                     | 6<br>7.              | 0<br>3.              | 1<br>3.                           | 5.<br>7                           | 0.<br>0      | 2.<br>3      | 6.<br>3      | 0.<br>6              | 2.<br>.             | 0.<br>1                          | 1<br>0            | 1.<br>8             | 2           | 1<br>0      | 1<br>0      | 1      | 3      | 2      | 1<br>0      | 2      | 8           | 3<br>7      | 2           | 3<br>0      | 1      | 3<br>6      | 4      | 7      | 3      | 2      | 9      | 7 |  |

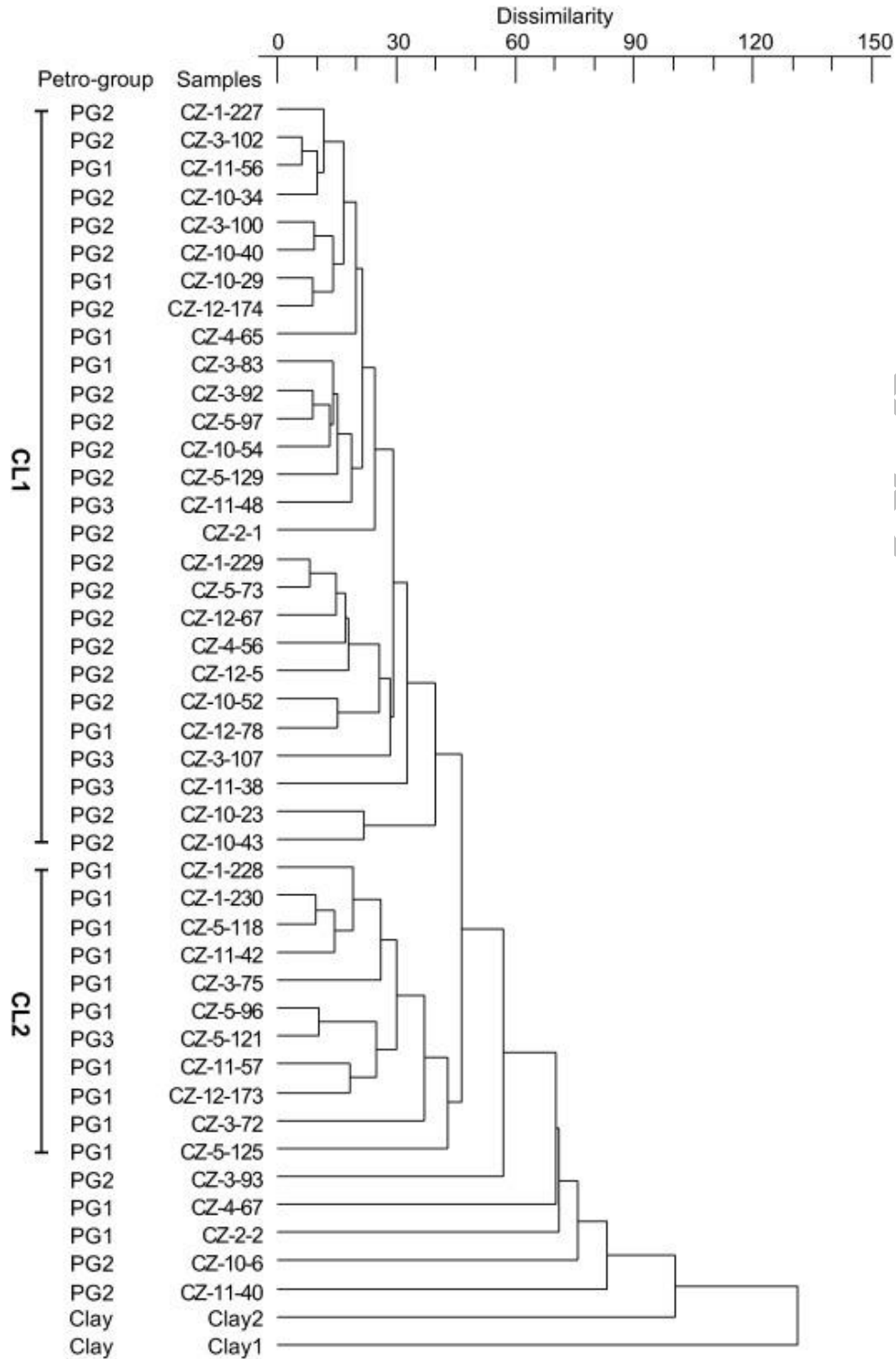
| Sa<br>m<br>pl<br>es      | Pet<br>ro-<br>gro<br>up | Si<br>O <sub>2</sub> | Ti<br>O <sub>2</sub> | Al <sub>2</sub><br>O <sub>3</sub> | Fe <sub>2</sub><br>O <sub>3</sub> | Mn<br>O  | Mg<br>O  | Ca<br>O  | Na <sub>2</sub><br>O | K <sub>2</sub><br>O | P <sub>2</sub><br>O <sub>5</sub> | Tot      | L.<br>O <sub>1</sub> | S<br>c   | V        | Cr | Co | Ni | Cu       | Zn | Ga       | Rb       | Sr | Y        | Zr | Nb       | Ba | La | Ce | Nd | Pb | Th | U |
|--------------------------|-------------------------|----------------------|----------------------|-----------------------------------|-----------------------------------|----------|----------|----------|----------------------|---------------------|----------------------------------|----------|----------------------|----------|----------|----|----|----|----------|----|----------|----------|----|----------|----|----------|----|----|----|----|----|----|---|
| 11<br>-<br>38            |                         | 89                   | 80                   | 67                                | 43                                | 39       | 29       | 42       | 45                   | 38                  | 01                               | 91       | 11                   | 77       | 00       | 50 | 00 | 88 | 16       | 88 | 88       | 77       | 00 | 66       | 66 | 16       | 66 | 55 | 33 |    |    |    |   |
| CZ<br>-<br>11<br>-<br>40 | PG<br>2                 | 65<br>24             | 08<br>33             | 14<br>21                          | 59<br>00                          | 09<br>04 | 29<br>07 | 66<br>05 | 06<br>01             | 27<br>07            | 01<br>05                         | 99<br>37 | 11                   | 22       | 10<br>44 | 16 | 32 | 31 | 82       | 24 | 82       | 33<br>33 | 26 | 28<br>22 | 16 | 36<br>01 | 38 | 65 | 42 | 88 | 14 | 77 |   |
| CZ<br>-<br>11<br>-<br>42 | PG<br>1                 | 64<br>62             | 08<br>88             | 15<br>65                          | 64<br>09                          | 07<br>04 | 27<br>01 | 56<br>04 | 06<br>09             | 26<br>09            | 01<br>06                         | 99<br>44 | 09<br>09             | 12<br>07 | 11<br>00 | 15 | 33 | 30 | 11<br>00 | 27 | 92       | 30<br>01 | 28 | 25<br>05 | 19 | 31<br>09 | 38 | 70 | 40 | 23 | 11 | 44 |   |
| CZ<br>-<br>11<br>-<br>48 | PG<br>3                 | 67<br>19             | 08<br>99             | 15<br>42                          | 58<br>07                          | 03<br>09 | 23<br>06 | 04<br>09 | 27<br>03             | 01<br>05            | 00<br>02                         | 16<br>03 | 16                   | 29       | 10<br>08 | 17 | 31 | 29 | 10<br>08 | 28 | 10<br>01 | 49<br>05 | 30 | 33<br>09 | 20 | 35<br>02 | 36 | 71 | 44 | 24 | 10 | 11 |   |
| CZ<br>-<br>11<br>-<br>56 | PG<br>1                 | 67<br>18             | 08<br>68             | 14<br>78                          | 58<br>03                          | 05<br>00 | 23<br>06 | 05<br>03 | 28<br>00             | 01<br>04            | 00<br>01                         | 18<br>03 | 11<br>08             | 11       | 10<br>05 | 18 | 31 | 30 | 10<br>07 | 24 | 10<br>00 | 39<br>06 | 32 | 35<br>05 | 18 | 36<br>01 | 56 | 75 | 40 | 23 | 11 | 44 |   |
| CZ<br>-<br>11<br>-<br>57 | PG<br>1                 | 64<br>97             | 08<br>54             | 14<br>94                          | 61<br>09                          | 06<br>05 | 27<br>00 | 06<br>07 | 27<br>05             | 01<br>02            | 00<br>01                         | 15<br>03 | 22                   | 11<br>07 | 10<br>08 | 18 | 33 | 26 | 11<br>00 | 26 | 93       | 34<br>05 | 31 | 28<br>04 | 18 | 33<br>00 | 41 | 60 | 36 | 26 | 99 | 66 |   |
| CZ<br>-<br>12<br>-<br>5  | PG<br>2                 | 68<br>04             | 07<br>88             | 12<br>83                          | 52<br>03                          | 03<br>01 | 24<br>07 | 06<br>02 | 25<br>03             | 01<br>01            | 09<br>05                         | 17<br>04 | 22                   | 10<br>06 | 95       | 14 | 26 | 27 | 88       | 22 | 91       | 30<br>09 | 29 | 38<br>01 | 16 | 36<br>01 | 43 | 63 | 38 | 22 | 99 | 88 |   |
| CZ<br>-<br>12<br>-<br>67 | PG<br>2                 | 68<br>47             | 08<br>56             | 13<br>66                          | 54<br>07                          | 03<br>01 | 28<br>01 | 07<br>01 | 27<br>07             | 01<br>03            | 00<br>01                         | 16<br>01 | 22                   | 10<br>05 | 99       | 16 | 28 | 26 | 10<br>06 | 22 | 90       | 40<br>00 | 32 | 43<br>08 | 18 | 36<br>05 | 44 | 65 | 36 | 25 | 88 | 11 |   |

| Sa<br>m<br>pl<br>es           | Pet<br>ro-<br>gro<br>up | Si<br>O <sub>2</sub> | Ti<br>O <sub>2</sub> | Al <sub>2</sub><br>O <sub>3</sub> | Fe <sub>2</sub><br>O <sub>3</sub> | Mn<br>O | Mg<br>O | Ca<br>O | Na <sub>2</sub><br>O | K <sub>2</sub><br>O | P <sub>2</sub><br>O <sub>5</sub> | Tot   | L<br>O <sub>i</sub> | S<br>c | V    | Cr   | Co   | Ni   | Cu    | Zn   | Ga   | Rb   | Sr   | Y    | Zr   | Nb   | Ba   | La   | Ce   | Nd   | Pb   | Th   | U |
|-------------------------------|-------------------------|----------------------|----------------------|-----------------------------------|-----------------------------------|---------|---------|---------|----------------------|---------------------|----------------------------------|-------|---------------------|--------|------|------|------|------|-------|------|------|------|------|------|------|------|------|------|------|------|------|------|---|
| CZ<br>-<br>12<br>-<br>78      | PG<br>1                 | 67.5                 | 0.81                 | 13.58                             | 5.60                              | 0.04    | 2.09    | 7.30    | 0.56                 | 2.55                | 0.14                             | 10.17 | 1.87                | 1.10   | 9.5  | 1.6  | 2.7  | 2.9  | 9.7   | 2.3  | 9.1  | 3.64 | 2.8  | 3.39 | 1.8  | 3.53 | 3.4  | 7.7  | 3.4  | 2.2  | 1.1  | 3    |   |
| CZ<br>-<br>12<br>-<br>17<br>3 | PG<br>1                 | 65.19                | 0.88                 | 15.68                             | 6.45                              | 0.05    | 2.47    | 5.11    | 0.55                 | 2.82                | 0.17                             | 9.37  | 2.11                | 1.25   | 1.18 | 1.8  | 3.6  | 3.2  | 10.9  | 2.6  | 9.9  | 2.91 | 3.0  | 2.65 | 1.8  | 3.25 | 3.9  | 7.3  | 5.2  | 3.0  | 1.1  | 3    |   |
| CZ<br>-<br>12<br>-<br>17<br>4 | PG<br>2                 | 67.51                | 0.89                 | 14.58                             | 5.80                              | 0.03    | 2.18    | 5.72    | 0.52                 | 2.70                | 0.14                             | 10.06 | 2.11                | 1.20   | 9.9  | 1.5  | 3.0  | 3.3  | 10.4  | 2.5  | 10.0 | 2.68 | 3.2  | 3.82 | 1.7  | 3.77 | 3.1  | 7.6  | 3.7  | 3.1  | 1.3  | 7    |   |
| CZ<br>-5-<br>11<br>8          | PG<br>1                 | 64.94                | 0.99                 | 15.86                             | 6.20                              | 0.03    | 2.78    | 5.58    | 0.89                 | 2.68                | 0.14                             | 9.92  | 0.99                | 1.26   | 1.13 | 1.6  | 3.3  | 2.7  | 11.2  | 2.7  | 9.7  | 3.05 | 2.9  | 2.75 | 2.1  | 3.02 | 4.1  | 7.1  | 4.3  | 2.5  | 9    | 3    |   |
| m<br>ea<br>n*                 |                         | 66.91                | 0.86                 | 14.03                             | 6.00                              | 0.03    | 2.31    | 5.45    | 0.60                 | 2.73                | 0.14                             | 9.97  | 1.67                | 1.13   | 1.04 | 1.55 | 1.83 | 2.81 | 10.38 | 2.49 | 9.56 | 3.49 | 2.97 | 3.25 | 1.78 | 3.81 | 3.9  | 7.36 | 3.4  | 2.2  | 1.0  | 4.39 |   |
| SD<br>*                       |                         | 1.61                 | 0.04                 | 1.03                              | 0.47                              | 0.03    | 0.30    | 1.20    | 0.11                 | 0.15                | 0.03                             | 0.31  | 0.09                | 0.34   | 0.95 | 0.82 | 1.70 | 0.65 | 3.71  | 1.87 | 1.66 | 1.48 | 1.87 | 5.01 | 1.37 | 5.71 | 7.90 | 5.67 | 5.99 | 4.21 | 2.24 | 2.39 |   |
| Sidi Zahrani n = 10           |                         |                      |                      |                                   |                                   |         |         |         |                      |                     |                                  |       |                     |        |      |      |      |      |       |      |      |      |      |      |      |      |      |      |      |      |      |      |   |
| m<br>ea<br>n*                 | Sidi<br>Za<br>hru<br>ni | 68.08                | 0.87                 | 14.90                             | 5.80                              | 0.05    | 1.97    | 4.74    | 0.50                 | 2.70                | 0.20                             | 9.86  | 1.14                | -      | 1.15 | 1.05 | 2.40 | 1.47 | 8.00  | 1.84 | 9.30 | 2.33 | 2.80 | 3.29 | 2.1  | 3.48 | -    | 8.16 | -    | 2.2  | 8.20 | -    |   |
| SD<br>*                       | Sidi<br>Za<br>hru       | 1.17                 | 0.04                 | 0.46                              | 0.09                              | 0.08    | 0.09    | 0.06    | 0.05                 | 0.00                | 0.03                             | 0.10  | 0.30                | -      | 0.49 | 0.50 | -    | 0.84 | 2.21  | 4.87 | 0.99 | 3.33 | 4.34 | 1.03 | 1.72 | 0.77 | 3.43 | -    | 4.33 | -    | 1.02 | 0.77 | - |



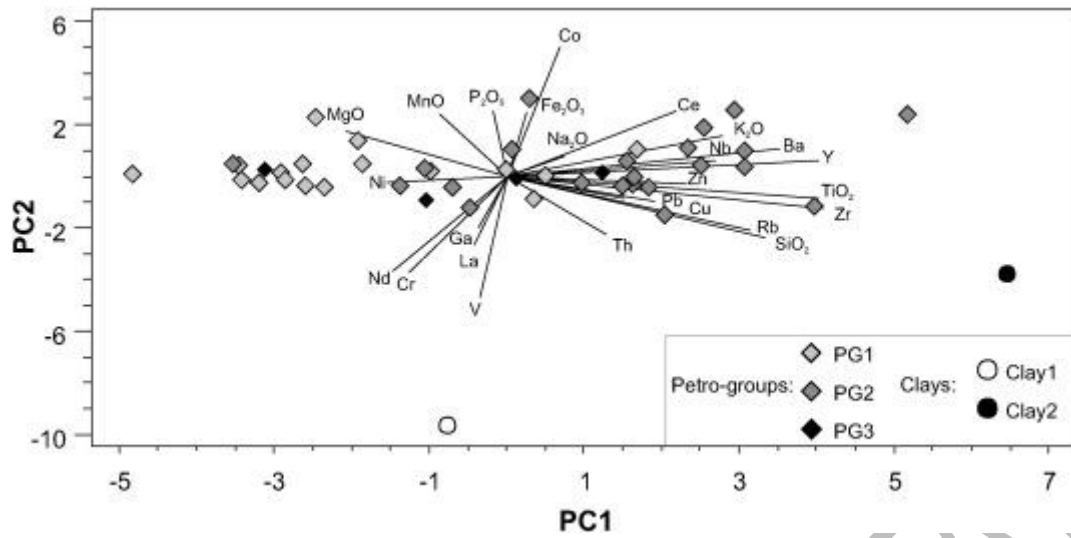
| Sa<br>m<br>pl<br>es        | Pet<br>ro-<br>gro<br>up       | Si<br>O <sub>2</sub> | Ti<br>O <sub>2</sub> | Al <sub>2</sub><br>O <sub>3</sub> | Fe <sub>2</sub><br>O <sub>3</sub> | Mn<br>O      | Mg<br>O      | Ca<br>O           | Na <sub>2</sub><br>O | K <sub>2</sub><br>O | P <sub>2</sub><br>O <sub>5</sub> | T<br>ot | L<br>O <sub>1</sub> | S<br>c | V           | Cr          | Co | Ni     | Cu     | Zn     | Ga     | Rb     | Sr          | Y      | Zr          | Nb     | Ba          | La | Ce     | Nd | Pb     | Th | U |
|----------------------------|-------------------------------|----------------------|----------------------|-----------------------------------|-----------------------------------|--------------|--------------|-------------------|----------------------|---------------------|----------------------------------|---------|---------------------|--------|-------------|-------------|----|--------|--------|--------|--------|--------|-------------|--------|-------------|--------|-------------|----|--------|----|--------|----|---|
|                            | ni                            |                      | 1                    |                                   |                                   |              |              |                   |                      | 8                   |                                  |         |                     |        |             |             |    |        |        |        |        |        | 5           |        | 1           | 8      | 0           |    | 2      |    | 2      | 8  |   |
| Nabeul area n = 7          |                               |                      |                      |                                   |                                   |              |              |                   |                      |                     |                                  |         |                     |        |             |             |    |        |        |        |        |        |             |        |             |        |             |    |        |    |        |    |   |
| CA<br>T2<br>21<br>CH<br>OG | Ch<br>ogg<br>afi<br>a         | 6<br>0.<br>7<br>9    | 0<br>.6<br>5         | 1<br>1.<br>0<br>7                 | 4.<br>2<br>5                      | 0.<br>0<br>2 | 1.<br>1<br>8 | 1<br>9.<br>0<br>1 | 0.<br>4<br>3         | 2<br>.0<br>7        | 0.<br>4<br>1                     | -       | -                   | -      | 1<br>0<br>5 | 1<br>1<br>1 | -  | 2<br>4 | 1<br>5 | 6<br>1 | 1<br>4 | 7<br>2 | 4<br>8<br>7 | 2<br>0 | 2<br>7<br>1 | 1<br>7 | 3<br>2<br>9 | -  | 5<br>9 | -  | 1<br>7 | 5  | - |
| CA<br>T2<br>32<br>LA<br>BA | La<br>bay<br>edh              | 6<br>9.<br>8<br>9    | 0<br>.7<br>4         | 1<br>4.<br>1<br>3                 | 5.<br>7<br>1                      | 0.<br>0<br>3 | 1.<br>9<br>5 | 4.<br>4<br>5      | 0.<br>4<br>8         | 2<br>.3<br>5        | 0.<br>1<br>4                     | -       | -                   | -      | 1<br>0<br>5 | 9<br>5      | -  | 2<br>6 | 1<br>0 | 6<br>7 | 1<br>6 | 7<br>5 | 1<br>9<br>2 | 2<br>0 | 1<br>7<br>8 | 1<br>8 | 2<br>2<br>8 | -  | 6<br>5 | -  | 1<br>8 | 6  | - |
| CA<br>T2<br>04<br>M<br>OK  | Mo<br>kni<br>ne               | 6<br>3.<br>0<br>3    | 0<br>.6<br>2         | 1<br>0.<br>9<br>2                 | 4.<br>0<br>1                      | 0.<br>0<br>3 | 1.<br>8<br>4 | 1<br>6.<br>6<br>9 | 0.<br>3<br>2         | 2<br>.2<br>8        | 0.<br>1<br>4                     | -       | -                   | -      | 1<br>0<br>4 | 8<br>8      | -  | 2<br>1 | 1<br>1 | 5<br>3 | 1<br>4 | 7<br>0 | 2<br>5<br>1 | 2<br>1 | 2<br>2<br>2 | 1<br>7 | 2<br>7<br>0 | -  | 6<br>0 | -  | 1<br>6 | 6  | - |
| CA<br>T2<br>20<br>M<br>OK  | Mo<br>kni<br>ne               | 6<br>1.<br>3<br>8    | 0<br>.6<br>6         | 1<br>2.<br>1<br>3                 | 4.<br>4<br>6                      | 0.<br>0<br>3 | 2.<br>1<br>4 | 1<br>6.<br>4<br>2 | 0.<br>2<br>5         | 2<br>.3<br>3        | 0.<br>2<br>4                     | -       | -                   | -      | 1<br>1<br>2 | 9<br>5      | -  | 2<br>5 | 1<br>4 | 6<br>8 | 1<br>6 | 7<br>4 | 2<br>4<br>1 | 2<br>4 | 2<br>3<br>5 | 1<br>8 | 3<br>3<br>2 | -  | 6<br>9 | -  | 1<br>8 | 7  | - |
| CA<br>T2<br>14<br>EC<br>H  | He<br>nch<br>ir<br>Che<br>kaf | 6<br>3.<br>4<br>6    | 0<br>.8<br>2         | 1<br>5.<br>0<br>1                 | 5.<br>6<br>8                      | 0.<br>0<br>4 | 2.<br>6<br>5 | 8.<br>8<br>4      | 0.<br>4<br>9         | 2<br>.5<br>5        | 0.<br>3<br>0                     | -       | -                   | -      | 1<br>2<br>2 | 1<br>1<br>3 | -  | 3<br>1 | 1<br>7 | 8<br>7 | 1<br>9 | 8<br>9 | 3<br>1<br>8 | 2<br>8 | 2<br>7<br>4 | 2<br>3 | 3<br>7<br>3 | -  | 8<br>2 | -  | 2<br>0 | 8  | - |
| CA<br>T2<br>24<br>EC<br>H  | He<br>nch<br>ir<br>Che<br>kaf | 6<br>1.<br>9<br>6    | 0<br>.8<br>4         | 1<br>5.<br>1<br>2                 | 5.<br>7<br>6                      | 0.<br>0<br>4 | 2.<br>8<br>4 | 1<br>0.<br>0<br>8 | 0.<br>6<br>2         | 2<br>.3<br>9        | 0.<br>2<br>1                     | -       | -                   | -      | 1<br>2<br>1 | 1<br>2<br>0 | -  | 3<br>1 | 1<br>5 | 7<br>7 | 1<br>8 | 8<br>2 | 2<br>7<br>9 | 2<br>7 | 2<br>6<br>1 | 2<br>1 | 2<br>9<br>6 | -  | 8<br>3 | -  | 1<br>9 | 7  | - |
| m<br>ea<br>n<br>CA<br>T    | He<br>nch<br>ir<br>Che<br>kaf | 6<br>3.<br>6<br>3    | 0<br>.8<br>1         | 1<br>4.<br>5<br>6                 | 5.<br>6<br>6                      | 0.<br>0<br>4 | 2.<br>5<br>6 | 9.<br>3<br>4      | 0.<br>5<br>3         | 2<br>.4<br>6        | 0.<br>2<br>8                     | -       | -                   | -      | 1<br>1<br>3 | 1<br>1<br>0 | -  | 3<br>1 | 1<br>3 | 7<br>7 | 1<br>7 | 7<br>8 | 2<br>5<br>7 | 2<br>5 | 2<br>5<br>0 | 2<br>1 | 2<br>7<br>9 | -  | 7<br>4 | -  | 1<br>7 | 8  | - |

| Sampl<br>es | Pet<br>ro-<br>gro<br>up | Si<br>O <sub>2</sub> | Ti<br>O <sub>2</sub> | Al <sub>2</sub><br>O <sub>3</sub> | Fe <sub>2</sub><br>O <sub>3</sub> | Mn<br>O | Mg<br>O | Ca<br>O | Na <sub>2</sub><br>O | K <sub>2</sub><br>O | P <sub>2</sub><br>O <sub>5</sub> | Tot  | L.<br>O·I | S<br>c | V   | C<br>r | C<br>o | N<br>i | C<br>u | Z<br>n | G<br>a | R<br>b | S<br>r | Y   | Z<br>r | N<br>b | B<br>a | L<br>a | C<br>e | N<br>d | P<br>b | T<br>h | U |
|-------------|-------------------------|----------------------|----------------------|-----------------------------------|-----------------------------------|---------|---------|---------|----------------------|---------------------|----------------------------------|------|-----------|--------|-----|--------|--------|--------|--------|--------|--------|--------|--------|-----|--------|--------|--------|--------|--------|--------|--------|--------|---|
| EC          |                         |                      |                      |                                   |                                   |         |         |         |                      |                     |                                  |      |           |        |     |        |        |        |        |        |        |        |        |     |        |        |        |        |        |        |        |        |   |
| Clays       |                         |                      |                      |                                   |                                   |         |         |         |                      |                     |                                  |      |           |        |     |        |        |        |        |        |        |        |        |     |        |        |        |        |        |        |        |        |   |
| Clay<br>1   | Clay1                   | 58.73                | 0.59                 | 9.82                              | 3.64                              | 0.02    | 1.33    | 2.35    | 0.34                 | 1.60                | 0.09                             | 9.96 | 2.05      | 1.01   | 7.9 | 6      | 2.4    | 2.6    | 7.3    | 1.8    | 6.8    | 7.1    | 1.9    | 2.6 | 1.1    | 2.3    | 4.3    | 3.8    | 3.7    | 1.9    | 9      | 4      |   |
| Clay<br>2   | Clay2                   | 71.46                | 0.79                 | 11.81                             | 5.43                              | 0.02    | 1.43    | 5.80    | 0.41                 | 2.44                | 0.09                             | 9.96 | 1.11      | 1.06   | 8.8 | 1      | 2.4    | 2.7    | 9.4    | 2.0    | 9.1    | 1.7    | 2.6    | 4.4 | 1.6    | 4.7    | 4.1    | 5.6    | 2.7    | 2.1    | 1.3    | 3      |   |



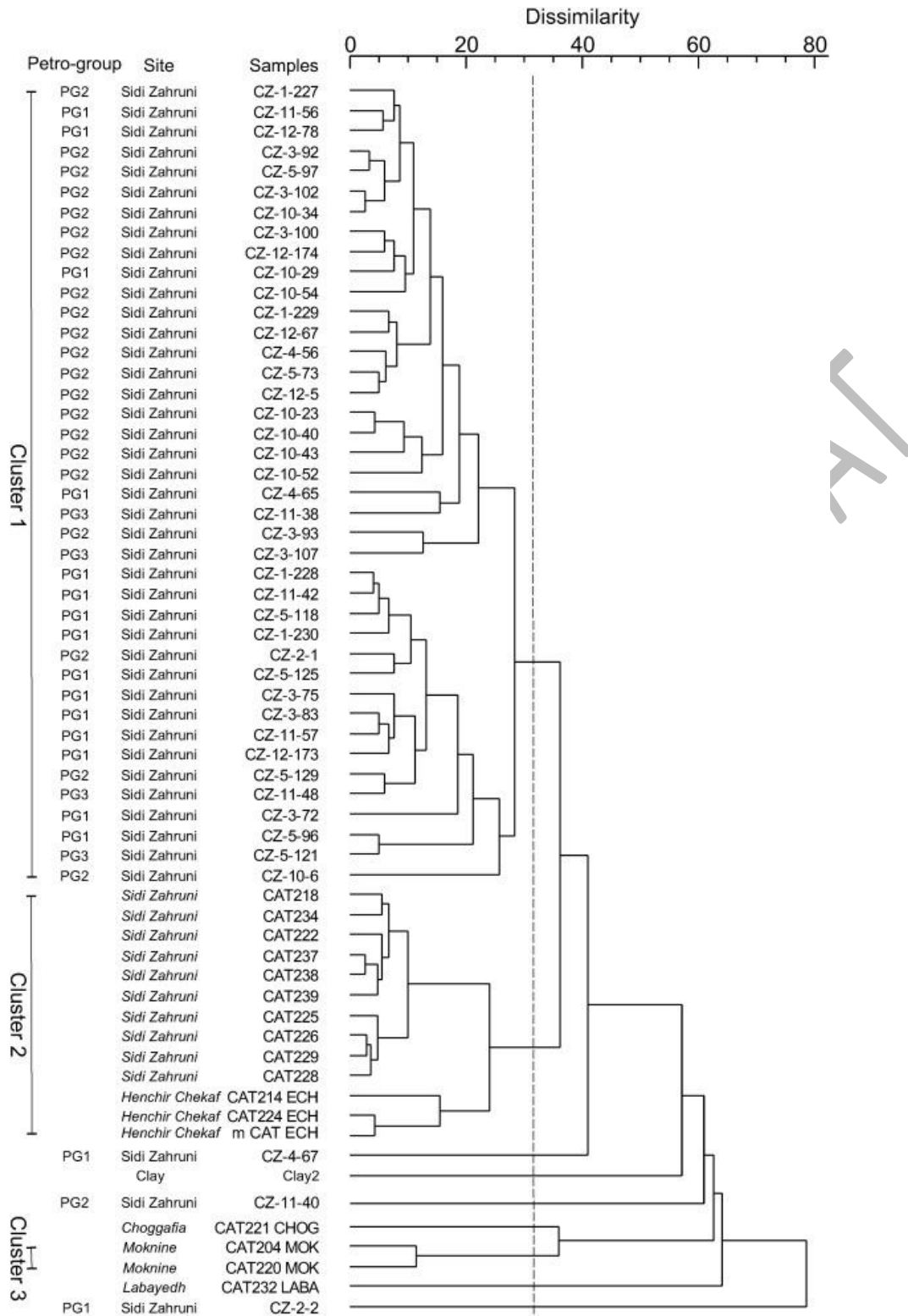
1. [Download high-res image \(562KB\)](#)
2. [Download full-size image](#)

Fig. 7. Dendrogram from hierarchic cluster analysis (average linkage method, square Euclidian distance) performed on sub-composition SiO<sub>2</sub>, TiO<sub>2</sub>, Fe<sub>2</sub>O<sub>3</sub>, MnO, MgO, Na<sub>2</sub>O, K<sub>2</sub>O, P<sub>2</sub>O<sub>5</sub>, V, Cr, Co, Ni, Cu, Zn, Ga, Rb, Y, Zr, Nb, Ba, La, Ce, Nd, Pb and Th, divided by Al<sub>2</sub>O<sub>3</sub>, for studied potsherds and clay materials. Abbreviations: CZ: amphorae from Sidi Zahruni site, AZ: clay materials collected near the site.



1. [Download high-res image \(215KB\)](#)
2. [Download full-size image](#)

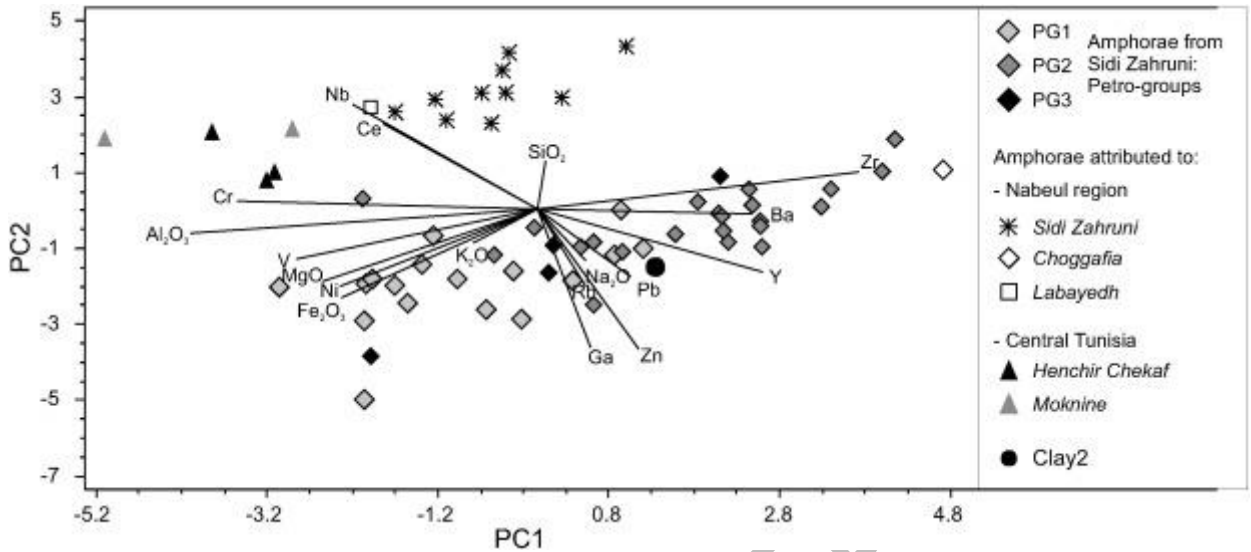
Fig. 8. Scores and loading plots of principal components 1 and 2 (PC1 vs. PC2) explaining 26% and 14% of total variance, respectively.



1. [Download high-res image \(1MB\)](#)
2. [Download full-size image](#)

Fig. 9. Dendrogram from hierarchic cluster analysis (average linkage method, square Euclidian distance) on sub-composition SiO<sub>2</sub>, Al<sub>2</sub>O<sub>3</sub>, Fe<sub>2</sub>O<sub>3</sub>, MgO, CaO, Na<sub>2</sub>O, K<sub>2</sub>O, V, Cr, Ni, Zn, Ga, Rb, Y, Zr, Nb, Ba, Ce and P divided by TiO<sub>2</sub>. CaO, Sr, MnO, Cu, P<sub>2</sub>O<sub>5</sub>, and Th were excluded from treatment due to their high ri:6.26, 4.03, 3.96, 3.20, 3, and 2.62, respectively. Amphorae from Sidi Zahruni analysed in this research and from other localities in north-eastern and central Tunisia are included. Samples

attributed to Sidi Zahrani, Henchir Chekaf, Moknine, Choggafia and Labayedh ([Fantuzzi et al., 2015a](#)) have the site name in *Italic*.



1. [Download high-res image \(298KB\)](#)
2. [Download full-size image](#)

Fig. 10. Scores and loading plots of principal components 1 and 2 (PC1 vs. PC2), representing 26% and 23% of total variance respectively, relative to PCA on amphorae from Sidi Zahrani and from other localities in north-eastern and central Tunisia. Sub-composition as in [Fig. 9](#).

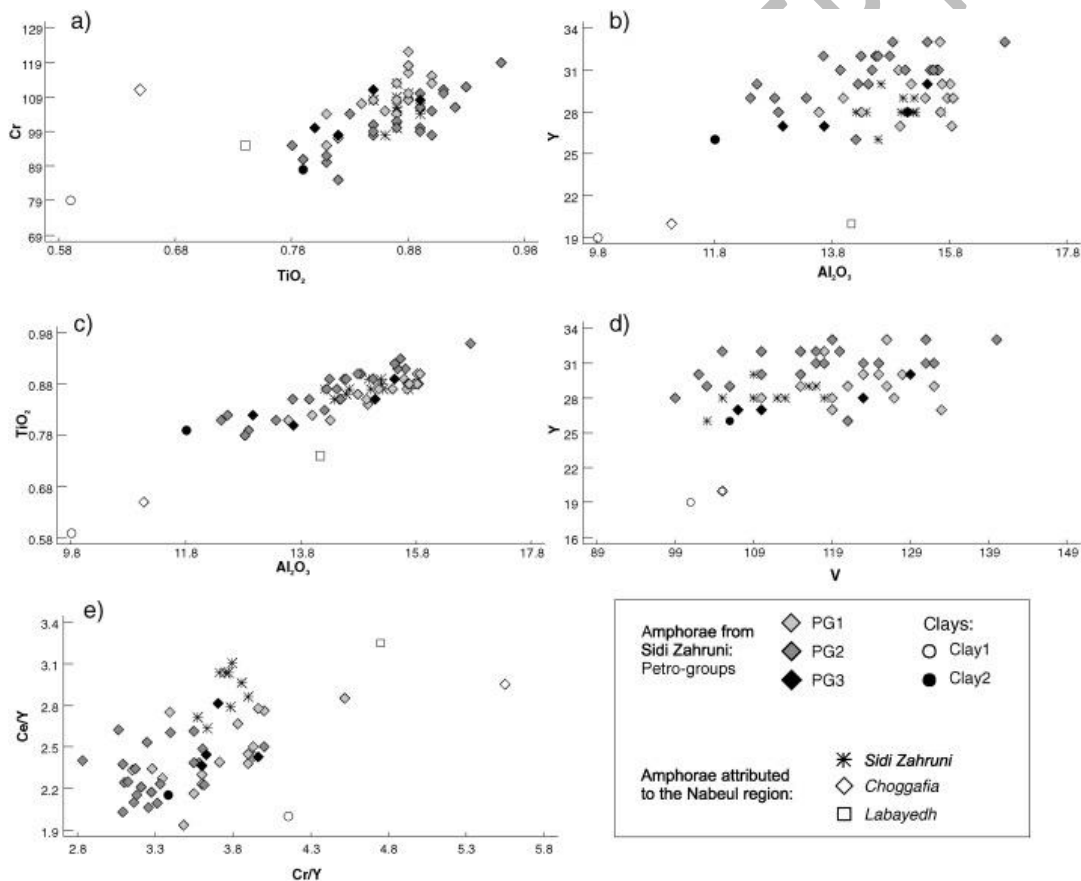
Separating the amphorae into two groups may reflect technological changes, since, the three production centres in the Nabeul region were active at different chronological phases: between the 2nd century and the first half of the 5th, amphorae were produced at Choggafia, and from the 5th to the 7th centuries at Sidi Zahrani and Labayedh ([Fantuzzi et al., 2015a,b](#) and references therein). This hypothesis does not exclude the possibility that the potters used various clay materials. According to Capelli and Bonifay ([Fantuzzi et al., 2015a,b](#) and references therein), the amphorae from Zahrani are more similar to those of Choggafia than those of Labayedh.

On the basis of these considerations, it cannot be excluded the possibility that differences between the amphorae found at Sidi Zahrani and those attributed to the site ([Fantuzzi et al., 2015a](#)) are due to the use of different clay materials or production processes. Since the inclusions are mainly composed of quartz and other major elements concentrations may have been affected by technological changes (addition of temper, levigation of clay), the trace element patterns of the amphorae should reflect those of the clay materials used ([Pillay et al., 2000](#)), therefore allowing us to constrain their provenance better ([Lee, 2002; Jia et al., 2004](#)). In this case study, one group of trace elements and two major potentially immobile elements (Y, Ce, Cr, V, Al, Ti) were selected to define possible sediment sources ([Bhatia and Crook, 1986; McLennan, 1992; Yang et al., 2003, 2004](#)).

Comparisons among potsherds from Sidi Zahrani, those attributed to the site, ones from other workshops in the Nabeul area and the clay materials collected near Sidi Zahrani all show that only one clay (Clay2) always overlaps with potsherds from

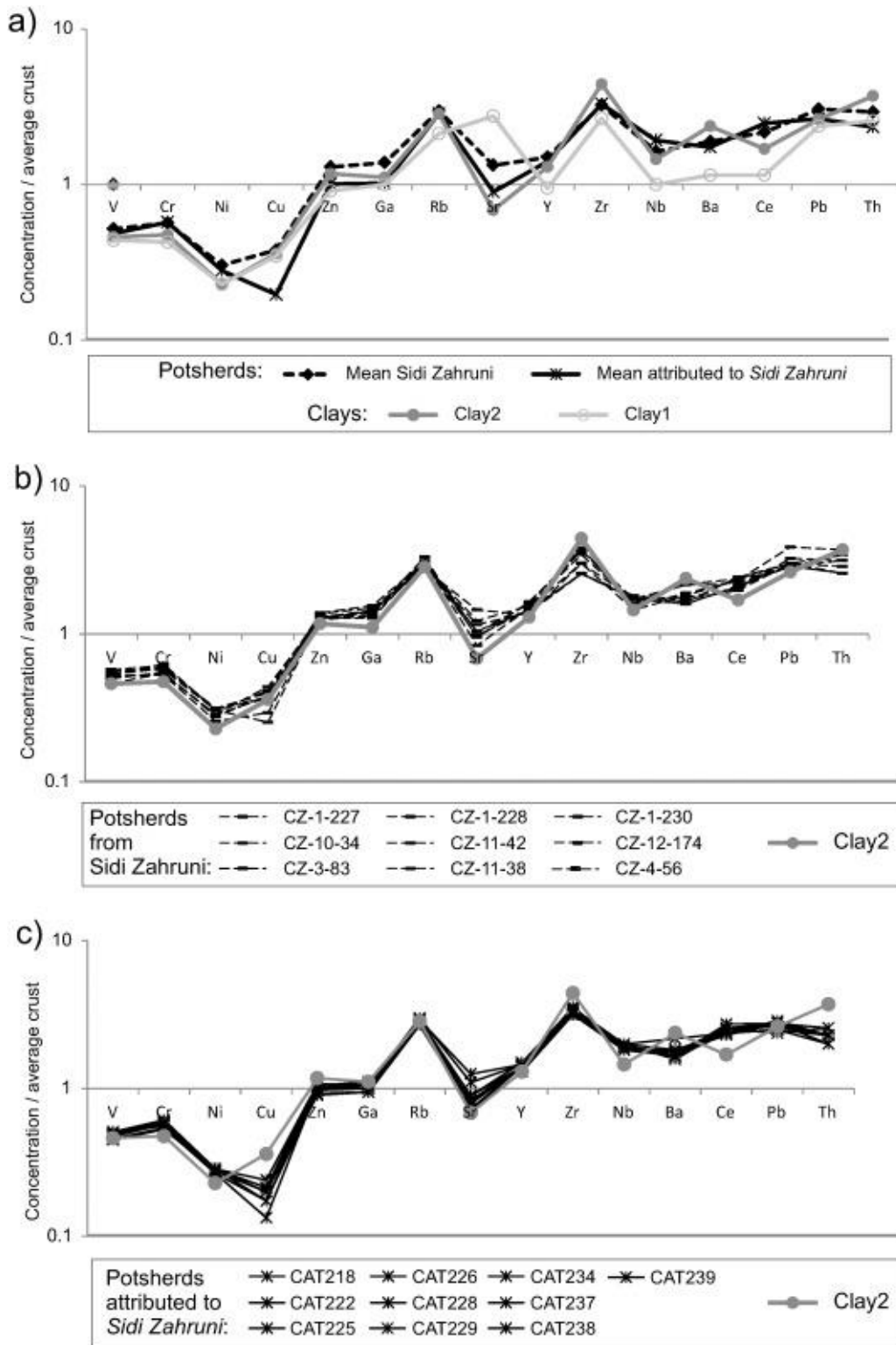


Sidi Zahrani and is attributed to the site, whereas the other (Clay1) is also isolated from the potsherds from Choggafia and Labayedh (Fig. 11). This indicates that the amphorae from the latter workshops were produced with a different clay material from that of Sidi Zahrani. Therefore, Clay2, collected from the Upper Miocene clay deposits of the Oued El Kebir formation, was most probably the one used to produce amphorae in the Sidi Zahrani workshop, independently of the type of the final product. This is also confirmed by the distribution of trace elements normalised to average continental crust, which demonstrates that the amphorae from Sidi Zahrani and those attributed to the site (Fantuzzi et al., 2015a) both show patterns very similar to those of Clay2 (Fig. 12). Small differences in some trace element concentrations, essentially between amphorae attributed to Sidi Zahrani and Clay2 (Fig. 12c), may reflect the small natural inhomogeneity of raw materials from the same geological formation along sedimentary clayey deposits. From an archaeological viewpoint, this is a satisfactory hypothesis: due to the longer production period of the centre (about 200 years), various levels from the same outcrop could have been exploited.



1. [Download high-res image \(490KB\)](#)
2. [Download full-size image](#)

Fig. 11. Binary variation diagrams of: a)  $\text{TiO}_2$  vs. Cr; b)  $\text{Al}_2\text{O}_3$  vs. Y; c)  $\text{Al}_2\text{O}_3$  vs.  $\text{TiO}_2$ ; d) V vs. Y; e) Ce/Y vs. Cr/Y for the amphorae from Sidi Zahrani, the clays collected near the site and the amphorae attributed by Fantuzzi et al. (2015a) to Sidi Zahrani, Choggafia and Labayedh.



1. [Download high-res image \(703KB\)](#)
2. [Download full-size image](#)

Fig. 12. Normalised elemental distribution of some trace and rare earth elements of: a) clay materials collected near Sidi Zahruni and average values of potsherds analysed in present work and attributed to *Sidi Zahruni* (italic) from [Fantuzzi et al. \(2015a\)](#); b) some selected potsherds from Sidi Zahruni here analysed and Clay2; c) the samples attributed to *Sidi Zahruni* from [Fantuzzi et al. \(2015a\)](#) and the Clay2.

Therefore, it can be established a new and consistent reference group of Keay 25.2 amphorae, together with those found in Catalonia by [Fantuzzi et al. \(2015a\)](#) according to their chemical composition, in view of available mineralogical and petrographic information, although some technological changes did occur.

## 6. Conclusions

This archaeometric study of Keay 25.2 amphorae from Sidi Zahruni (north-eastern Tunisia) based on petrographic and mineralogical compositions provided significant information to describe the nature of this ceramic class.

Petrographically, all samples were very similar, with small differences in the textural features of the inclusions revealed by image analysis. The different proportions between matrix and inclusions, especially quartz, are responsible for the small geochemical differences among the samples. Also from a mineralogical viewpoint, the amphorae from Sidi Zahruni are homogeneous, indicating standardised production technology in terms of source clay, paste preparation and firing conditions. Geochemical comparisons with a group of African amphorae found in Tarragona (Spain) and attributed to the Sidi Zahruni workshop indicates that different variants of amphorae produced at Sidi Zahruni are similar, especially in terms of trace element patterns, indicating that the same clay source was used for these productions. In more detail, the amphorae produced at Sidi Zahruni were made from the clay outcropping in the nearby Upper Miocene deposits of the Chabat Al Qola. The availability of large quantities of raw materials would have been an obvious factor in locating a flourishing ceramic industry in the Nabeul area. The different geochemical composition of the amphorae produced in other workshops in the area indicates that the potters followed their own production strategies and used different base clays.

A new and consistent reference group for the Keay 25.2 amphorae from Sidi Zahruni is now established, and is also representative of the various fabrics found at the site. This reference group will be useful for further provenance studies on Roman amphorae, to identify possible exportation from Sidi Zahruni to other sites, especially in Hispania, where the Keay 25.2 type of amphora has often been found, and to better define how this type spread and where it was imitated. Such data will aid interpretation of the socio-economic relations between various regions, trade routes and the technological evolution of societies.

## Acknowledgements

The authors would like to thank the Institute of Patrimony of Tunis (INP) for providing access to the archaeological site of Sidi Zahruni. They are also very grateful to G. Walton, who revised the English text, and two anonymous referees and Faiza Bergaya, whose comments improved the manuscript. This research is part of ongoing collaboration between the Unité de Recherche: Pétrologie cristalline et sédimentaire (Université Tunis El Manar), the Department of Geosciences of the University of Padova (Italy) and the Geology Department of the Universitat Autònoma de Barcelona (Spain). It benefited by funding from the University of Padova (Erasmus Mundus Al-IDRISI II scholarship and International cooperation), from the Spanish Ministerio de Economía y Competitividad (project

[CGL2013-42167](#)) and from technical and human resources of the Faculty of Sciences of the University of Tunis.

## References

- [Baxter, 1994](#)  
M.J. Baxter **Exploratory Multivariate Analysis in Archaeology**  
University Press, Edinburgh (1994)
- [Baxter, 1999](#)  
M.J. Baxter **Detecting multivariate outliers in artefact compositional data**  
*Archaeometry*, 41 (1999), pp. 321-338
- [Bes, 2007](#)  
Bes, P., 2007. A Geographical and Chronological Study of the Distribution and Consumption of Tableware in the Roman East, Leuven, Unpublished PhD thesis, Katolieke Universiteit Leuven.
- [Bhatia and Crook, 1986](#)  
M.R. Bhatia, A.W. Crook **Trace element characteristics of graywackes and tectonic setting discrimination of sedimentary basins**  
*Contrib. Mineral. Petrol.*, 92 (1986), pp. 181-193
- [Buxeda i Garrigós, 1999](#)  
J. Buxeda i Garrigós **Alteration and contamination of archaeological ceramics: the perturbation problem**  
*J. Archaeol. Sci.*, 26 (1999), pp. 295-313  
[ArticlePDF \(365KB\)](#)
- [Buxeda i Garrigós et al., 2002](#)  
J. Buxeda i Garrigós, M. Comas i Solà, J.M. Gurt i Esparraguera **Roman amphorae production in Baetulo (Badalona, Catalonia). Evidence of Pascual 1**  
V. Kilikoglou, A. Heinand, Y. Maniatis (Eds.), *Modern Trends in Scientific Studies on Ancient Ceramics*, BAR International Series, Vol. S1011 (2002), pp. 277-285 (Oxford)
- [Capelli, 2005](#)  
C. Capelli **Tunisian Fabric in Roman Amphorae: A Digital Resource (University of Southampton)**  
Archaeology Data Service, York (2005), [10.5284/1000021](#)
- [Capelli and Leitch, 2011](#)  
C. Capelli, V. Leitch **A Roman amphora production site near Lepcis Magna: petrographic analyses of the fabrics**  
*Libyan Stud.*, 42 (2011), pp. 69-72
- [Cultrone et al., 2004](#)  
G. Cultrone, E. Sebastián, K. Elert, M.J. de la Torre, O. Cazalla, C. Rodriguez-Navarro **Influence of mineralogy and firing temperature in the porosity of bricks**  
*J. Eur. Ceram. Soc.*, 34 (2004), pp. 547-564  
[ArticlePDF \(856KB\)](#)
- [Dal Sasso et al., 2014](#)  
G. Dal Sasso, L. Maritan, S. Salvatori, C. Mazzoli, G. Artioli **Discriminating pottery production by image analysis: a case study of Mesolithic and Neolithic pottery from Al Khiday (Khartoum, Sudan)**  
*J. Archaeol. Sci.*, 46 (2014), pp. 125-143  
[ArticlePDF \(8MB\)](#)
- [Dias et al., 2010](#)

- M.I. Dias, M.I. Prudêncio, M.A. Gouveia, M.J. Trindade, R.A. Marques, D. Franco, J. Raposo, C.S. Fabião, A. Guerra **Chemical tracers of Lusitanian amphorae kilns from the Tagus estuary (Portugal)**  
J. Archaeol. Sci., 37 (2010), pp. 784-798  
[ArticlePDF \(1MB\)](#)
- [Fantuzzi et al., 2015a](#)  
L. Fantuzzi, M.A. Cau Ontiveros, J.M. Macias **Amphorae from the late antique city of Tarraco-Tarracona (Catalonia, Spain): archaeometric characterisation**  
Period. Mineral. Spec. Issue, 84 (2015), pp. 169-212
  - [Fantuzzi et al., 2015b](#)  
L. Fantuzzi, M.A. Cau Ontiveros, X. Aquilué **Archaeometric characterization of amphorae from late Antique City of Emporiae (Catalonia, Spain)**  
Archaeometry (2015), [10.1111/arc.12176](#)
  - [Fermo et al., 2008](#)  
P. Fermo, E. Delnevo, M. Lasagni, S. Polla, M. De Vos **Application of chemical and chemometric analytical techniques to the study of ancient ceramics from Dougga (Tunisia)**  
Microchem. J., 88 (2008), pp. 150-159  
[ArticlePDF \(3MB\)](#)
  - [Govindaraju, 1994](#)  
K. Govindaraju **Compilation of working values and sample description for 383 geostandards**  
Geostand. Newslett., 18 (Special Issue) (1994), pp. 1-158
  - [Grifa et al., 2009](#)  
C. Grifa, G. Cultrone, A. Langella, M. Mercurio, A. De Bonis, E. Sebastián, V. Morra **Ceramic replicas of archaeological artefacts in Benevento area (Italy): Petrophysical changes induced by different proportions of clays and temper**  
Appl. Clay Sci., 46 (2009), pp. 231-240  
[ArticlePDF \(792KB\)](#)
  - [Gualtieri et al., 1995](#)  
A. Gualtieri, M. Bellotto, G. Artioli, M. Clark **Kinetic study of the kaolinite-mullite reaction sequence. Part II: mullite formation**  
Phys. Chem. Miner., 22 (1995), pp. 215-222
  - [Jia et al., 2004](#)  
X. Jia, J. Dong, S. Han, Y. Tang, Z. Gao **INAA analysis for Jun porcelain and modern Chinese Jun porcelain**  
J. Isot., 17 (2004), pp. 129-134
  - [Keay, 1984](#)  
S.J. Keay **Late Roman Amphorae in the Western Mediterranean. A Typology and Economic Study: The Catalan Evidence**  
Bar International Series, Vol. 196 (1984)  
(738 pp.)
  - [Lee, 2002](#)  
Y. Lee **Provenance derived from the geochemistry of late Paleozoic-early Mesozoic mudrocks of the Pyeongan Supergroup, Korea**  
Sediment. Geol., 149 (2002), pp. 219-235  
[ArticlePDF \(320KB\)](#)
  - [Maritan et al., 2005](#)  
L. Maritan, C. Mazzoli, L. Nodari, U. Russo **Second Iron age grey pottery from Este (north-eastern Italy): study of provenance and technology**  
Appl. Clay Sci., 29 (2005), pp. 31-44  
[ArticlePDF \(441KB\)](#)
  - [Maritan et al., 2006](#)

- L. Maritan, L. Nodari, C. Mazzoli, A. Milano, U. Russo **Influence of firing conditions on ceramic products: experimental study on clay-rich inorganic matter**  
Appl. Clay Sci., 31 (2006), pp. 1-15  
[ArticlePDF \(561KB\)](#)
- [Maritan et al., 2015](#)  
L. Maritan, P. Holakoei, C. Mazzoli **Cluster analysis of XRPD data in ancient ceramics: what for?**  
Appl. Clay Sci., 114 (2015), pp. 540-549  
[ArticlePDF \(906KB\)](#)
  - [McLennan, 1992](#)  
S.M. McLennan **Continental crust**  
W.A. Nierenberg (Ed.), Encyclopedia of Earth Sciences, Kluwer, Dordrecht (1992), pp. 581-592
  - [Nodari et al., 2007](#)  
L. Nodari, E. Marcuz, L. Maritan, C. Mazzoli, U. Russo **Hematite nucleation and growth in the firing of carbonate-rich clay for pottery production**  
J. Eur. Ceram. Soc., 27 (2007), pp. 4665-4673  
[ArticlePDF \(1MB\)](#)
  - [Peacock, 1984](#)  
D.P.S. Peacock **Petrology and Origins**  
M.G. Fulford, D.P.S. Peacock (Eds.), Excavations at Carthage: The British Mission, Vol. I, 2, the Avenue Du Président Habib Bourguiba, Salambo: The Pottery and Other Ceramic Objects from the Site, Sheffield, British Academy/University of Sheffield (1984), pp. 6-20
  - [Peacock, 1994](#)  
D.P.S. Peacock **The amphorae: typology, fabric and chronology**  
M.G. Fulford, D.P.S. Peacock (Eds.), Excavation at Carthage, The British Mission, II, Vol. 2 (1994), pp. 42-52
  - [Peacock and Tomber, 1991](#)  
D.P.S. Peacock, R. Tomber **Roman amphora Kilns in the Sahel of Tunisia: petrographic investigation of Kiln material from a sedimentary environment**  
A. Middleton, I. Freestone (Eds.), Recent Developments in Ceramic Petrology, Occasional Paper 81, British Museum, London (1991), pp. 289-304
  - [Peacock et al., 1989](#)  
D.P.S. Peacock, F. Bejaoui, N. Belazreg **Roman amphora production in the Sahel Region of Tunisia**  
M. Lenoir, D. Manacorda, C. Panella (Eds.), Amphores Romaines et Histoire Économique. Dix Ans de Recherche, Actes Du Colloque de Sienne (22-24 Mai 1986), École Française de Rome, Rome (1989), pp. 180-222
  - [Peacock et al., 1990](#)  
D.P.S. Peacock, F. Béjaoui, N. Ben Lazreg **Roman pottery production in Central Tunisia**  
JRA, 3 (1990), pp. 59-84
  - [Pillay et al., 2000](#)  
A.E. Pillay, C. Punyadeera, L. Jacobson, J. Eriksen **Analysis of ancient pottery and ceramic objects using X-ray fluorescence spectrometry**  
X-Ray Spectrom., 29 (2000), pp. 53-62
  - [Piovesan et al., 2013](#)  
R. Piovesan, C. Dalconi, L. Maritan, C. Mazzoli **X-ray powder diffraction diagram clustering and quantitative phase analysis on historic mortars**  
Eur. J. Mineral., 25 (2013), pp. 165-175
  - [Prudêncio et al., 2003](#)



M.I. Prudêncio, M.I. Dias, J. Raposo, M.A. Gouveia, C. Fabião, A. Guerra, J. Bugalhão, A.L. Duarte, A. Sabrosa **Chemical characterisation of amphorae from the Tagus and Sado Estuaries Production Centres (Portugal)**

S. Di Pierro, V. Serneels, M. Maggetti (Eds.), *Ceramic in the Society*, Proceedings of the EMAC'01, Fribourg (2003), pp. 245-253

- [Prudêncio et al., 2009](#)  
M.I. Prudêncio, M.I. Dias, M.A. Gouveia, R. Marques, D. Franco, M.J. Trindade **Geochemical signatures of Roman amphorae produced in the Sado River estuary, Lusitania (western Portugal)**  
*J. Archaeol. Sci.*, 36 (2009), pp. 873-883  
[ArticlePDF \(888KB\)](#)
- [Schuring, 1984](#)  
J.M. Schuring **Studies on Roman amphorae I-II**  
*BABesch*, 59 (1984), pp. 137-195
- [Sherriff et al., 2002a](#)  
B.L. Sherriff, P. Court, S. Johnston, L. Stirling **The source of raw materials for Roman pottery from Leptiminus, Tunisia**  
*Geoarchaeology*, 17 (2002), pp. 835-861
- [Sherriff et al., 2002b](#)  
B.L. Sherriff, C. Mc Cammon, L. Stirling **A Mössbauer study of the color of Roman pottery from the Leptiminus archaeological site, Tunisia**  
*Geoarchaeology*, 17 (2002), pp. 863-874
- [Vitali and Franklin, 1986](#)  
V. Vitali, U.M. Franklin **New approaches to characterization and classification of ceramics on the basis of their elemental composition**  
*J. Archaeol. Sci.*, 13 (1986), pp. 161-170  
[ArticlePDF \(825KB\)](#)
- [Whitbread, 1989](#)  
I.K. Whitbread **A proposal for the systematic description of thin sections towards the study of ancient ceramic technology**  
*Proceedings of the 25th International Symposium on Archaeometry*, Elsevier (1989), pp. 127-138
- [Whitbread, 1995](#)  
I.K. Whitbread **Greek transport amphorae: a petrological and archaeological study**  
*Fitch Laboratory Occasional Paper*, Vol. 4, School at Athens, British (1995)
- [Whitney and Evans, 2010](#)  
D.L. Whitney, B.W. Evans **Abbreviations for names of rock-forming minerals**  
*Am. Mineral.*, 95 (2010), pp. 185-187
- [Yang et al., 2003](#)  
S.Y. Yang, C.X. Li, C.B. Lee, T.K. Na **REE geochemistry of suspended sediments from the rivers around the Yellow Sea and provenance indicators**  
*Chin. Sci. Bull.*, 48 (2003), pp. 1135-1139
- [Yang et al., 2004](#)  
S.Y. Yang, D.I. Lim, H.S. Jung, B.C. Oh **Geochemical composition and provenance discrimination of coastal sediments around Cheju Island in the south-eastern Yellow Sea**  
*Mar. Geol.*, 206 (2004), pp. 41-53  
[ArticlePDF \(949KB\)](#)